



JOURNAL OF MACROMOLECULAR SCIENCE®

Part B—Physics

Vol. B42, No. 1, pp. 1–56, 2003

Construction of the Full Phase Diagram for the System of Poly(γ -benzyl-L-glutamate)/Dimethylformamide on the Basis of the Complex of Literature Data[†]

Boris M. Ginzburg* and Andrej A. Shepelevskii

Institute of Problems of Mechanical Engineering, Russian Academy of Sciences,
St. Petersburg, Russia

ABSTRACT

The system poly- γ -benzyl-L-glutamate—dimethylformamide (PBG/DMF) is the most-studied of the rodlike polymer-solvent systems. However, up to now there is no satisfactory experimental phase diagram (PD) for this system in the entire range of concentrations. For all studied systems only fragments of the PD are known. Some regions of these fragments agree qualitatively with the theoretical PD for an ensemble of rodlike particles in an isotropic solvent. However, most parts of the PD do not agree with the theoretical ones. A critical analysis of the corresponding experimental data was carried out and on the basis of this analysis a new PD was constructed in the entire range of concentration. The obtained PD differs essentially from the known theoretical diagram and is very close to the diagram predicted by Papkov taking into account the formation of crystallo-solvates. The peculiarities of the phase transitions in the various regions of the PD are considered. It is shown that the so-named lyotropic liquid crystals (LC), on the basis of solved rodlike polymers, are thermotropic LCs diluted by the isotropic solvent. A specific role in the PD are played by the crystallo-solvates (CS), which are identified with the phase defined by Luzzati as the “complex phase.” In particular, the phase region LC-CS exists instead of the LC-LC

[†]Dedicated to Paul Flory's memory.

*Correspondence: Boris M. Ginzburg, Institute of Problems of Mechanical Engineering, Russian Academy of Sciences, Bolshoi pr., 61, V.O. St. Petersburg 199178, Russia; E-mail: ginzburg@tribol.ipme.ru.

region in the theoretical PDs. Some new concepts of the crystallosolvate defects and on the “limiting” LC phase are discussed. Consideration of the liquidus lines CS/LC and CS/(isotropic liquid) permits us to propose some explanations of the PDs at low polymer concentrations. Most parts of the real PD represent the superposition of different phase equilibria and are complicated by the processes of gelation, crystallization and crystallosolvate formation that cannot be described by the modern theories. The fragments of the PDs in the literature for some rodlike polymers in solution agree well with the general PD for PBG/DMF. Special features of the phase transitions in the different areas of the PD are discussed. On the basis of the principles used in this work for construction of the PD, critical consideration of the PDs published in the literature have been carried out; our understanding of results obtained by other authors are presented. The perspectives of further investigations are considered.

Key Words: Polymer; Liquid crystal; Phase diagram; Gel; Crystallosolvate; Poly(γ -benzyl-L-glutamate).

1. INTRODUCTION

Construction of the phase diagram (PD) of polymer solutions capable of forming a liquid crystal (LC) state is an important direction in the investigation of these systems (see, e.g., Refs.^[1-4]). This is due both to scientific interest in the polymer LC state, and of the application significance of the corresponding results. Thus, from LC polymer solutions high strength and high modulus fibers have been obtained^[5-7]; from polymer LC systems with polymerizable solvent anisotropic plastics have been obtained saving the LC structure of the initial solution^[8-11]; LC polymer solutions have been used for preparation of highly selective membranes,^[12] including membranes from block copolymers with mesogenic blocks^[13]; many biological systems operate in the LC solution state,^[14,15] etc.

This is, naturally, far from the complete list of possible applications, but independently of its length, knowledge of the PD of the system used is undeniably necessary in all cases for its employment. In this work we will consider the system of a rigid-chain polymer/isotropic solvent as an example of polymer bicomponent systems that can form a liquid crystal state. We suppose, however, that the problem raised in this paper has a direct bearing on all polymers capable of forming thermotropic liquid crystals and simultaneously to be soluble in an isotropic solvent.

First of all we keep in mind that all thermotropic LC polymers are constructed with a “mesogen attached to a spacer” in the main or side chain. We suppose that the PDs of the temperature-composition type for binary systems from this type of polymers and solvents will have one of the shapes described in this work. This is natural because the phase state of these polymers, as in the case of rigid-chain polymers, can be described by an ensemble of rigid rods.

The systems PBG-solvent are one of the most comprehensively studied model polymer systems with LC structure (see, e.g., reviews^[16-18] and monograph^[19]). This is caused not only by a detailed knowledge of molecular properties of the polymer but also by the uniqueness of the properties of its LC systems, and by accessibility to investigation of these systems with comparatively simple experimental methods. The systems PBG-solvent



Phase Diagram for System of PBG/DMF

3

have become classic model subjects and results of their investigations have a general significance for the rigid-chain polymer/solvent systems, capable of forming a mesophase.

For the studies of PBG solutions the most frequently used solvents have been dimethylformamide (DMF), dioxane, m-cresol, dichloromethane, dichloroacetic acid, and some others.

However, despite the variety of studies of PBG solutions, both in the isotropic state and in an LC state, our knowledge of the PD of these systems was far from complete until recently. With reliability, only some parts of the PD were obtained. At the same time there are many separate works in the literature not devoted directly to the construction of the PD but nevertheless such that their common consideration and analysis can be used for this construction.

In the present paper a critical analysis of the experimental data of different authors about the PD of the system PBG/DMF is carried out. On the basis of this analysis the real PD is constructed for the indicated system for all possible concentrations. The constructed PD significantly differs from all known PD for this polymer up to the present time. Its shape qualitatively agrees well with a hypothetical PD, proposed by Papkov for solutions of rigid-chain polymers taking into account the superposition of various phase equilibria and possible formation of LC and crystallosolvates.^[3,16,17] In addition special features of the phase transitions in various areas of the PD will be considered.

In Section 1 some general characteristics of the main components of the considered system, PBG and DMF, will be briefly given. The most important results of theoretical studies of PDs of rodlike macromolecules are outlined in Section 2. In Section 3 literature experimental data relating to temperature and concentration transitions in the systems PBG-solvent and other experimental data concerning the structure and properties of these systems and physical interpretation of mentioned transitions will be considered. In Section 4 it is shown how to construct the generalized PD for the PBG-DMF system in the entire concentration range on the basis of the data considered in the previous sections. A significantly new feature is the existence of the crystallosolvate (CS) phase. The availability of this phase can explain many special peculiarities of the system and its PD. This classification introduces a new structure unit for the system with the possibility of defects of the CS phase. Wherever it is possible, analogous behavior and properties of other systems of rodlike polymer-isotropic solvent will be discussed. Based on the principles, used in this work for construction of the PDs, critical consideration of PD published in the literature has been carried out; our understanding of results obtained by other authors will be presented. The perspectives of further investigations are considered.

2. GENERAL CHARACTERISTICS OF THE PBG-DMF SYSTEM

The synthetic polypeptide PBG has the following chemical structure for its repeat unit: $(-\text{NHCH}(\text{R})\text{CO}-)_n$, where $\text{R} = -(\text{CH}_2)_2 \text{C}(\text{O})\text{OCH}_2\text{C}_6\text{H}_5$. Since the discovery of Elliot and Ambrose,^[20] detecting a liquid anisotropic phase formed upon evaporation of a PBG solution in chloroform, PBG solutions have been widely used as model systems both for studies of the PD of rodlike polymers and for investigation of the nature of the polymeric LC state. This is due to several reasons.

First, Robinson^[21,22] showed that the anisotropic phase of PBG solutions can form not only in chloroform, but in many other solvents as well, in all cases represented by LC of the cholesteric type. By a series of works^[21–24] devoted to the LC state of PBG solutions Robinson attracted the wide attention of researchers to the PBG/solvent systems.

Second, almost simultaneously with Robinson's experimental works the theoretical works of Onsager^[25] and Ishihara^[26] appeared, devoted to the properties of athermal solutions of rodlike particles; they predicted the dependencies of some main parameters of LC systems—so-called “critical concentrations”—on the axial or aspect ratio of the rods $x = L/D$, where L and D are the length and diameter of the rodlike particles. Shortly after this, some theoretical works of Flory were published.^[27,28] In the Flory theory, for the same systems of rods in solvent, not only critical concentrations were predicted but also—and what is especially important—the shape of the PD in the χ versus V_2 coordinates, where χ is the Flory-Huggins interaction parameter and V_2 is the concentration (or the volume fraction) of the rodlike particles. Because the parameter χ is a single-valued function of the temperature T ^[29] the theoretical PD can be verified experimentally in T versus V_2 coordinates.

Thirdly, by synthesizing PBG of various molecular mass (MM), i.e., varying the rod length, it was possible to change the aspect ratio without significant change of the polymer-solvent interaction. Then it was possible to study the influence of x and x -polydispersity on the different properties of LC systems (for example, see Refs.^[22,30]).

Fourth, the specific helix structure of cholesteric LC systems allows a very easy and convenient method to identify the LC state and detect its changes in response to an external action; it can be made by usual optical methods, mainly by polarized light microscopy and by small-angle diffraction of polarized light.

This permits the use of LC solutions of PBG for studying the effects of temperature, concentration, solvent nature, and other physicochemical factors (e.g., Refs.^[21,22,30–34]), and of electric and magnetic fields (e.g., Refs.^[35–40]) on the cholesteric structure.

Also the LC solutions of PBG are very convenient objects for studying by other techniques as can be seen from the cited reviews.

We note that there are two possible conformations adopted by PBG molecule in solution: α -helix and random coil. The LC state appears only in the PBG solutions featuring the α -helix conformation. Only in this case can the PBG molecule be modeled by a rigid rod (that is important for the forming of LC state) and in this case it can be considered as a rigid chain polymer.

Figure 1 shows a schematic diagram of the rodlike structure of PBG molecules, representing a right-handed α -helix.^[41–45] By analogy with Ref.^[46], this diagram illustrates various possibilities of selecting the molecular diameter D for calculating the x value.

Note that the side chains of PBG exhibit a rather autonomous behavior. In particular, they form, together with the side chains of neighboring molecules, slightly tilted stacks of benzene rings.^[47] This stacking creates a kind of external spiral groove with respect to the backbone. The pitch of this groove differs sharply from the pitch of the α -helix and determines the chirality of the cholesteric helix.^[48]

The groove tilt depends on the temperature and can change its sign to the opposite one. This determines a unique temperature dependence of the pitch for cholesteric LC in PBG solutions. This is reflected in the fact that the temperature dependence of the chiral

Phase Diagram for System of PBG/DMF

5

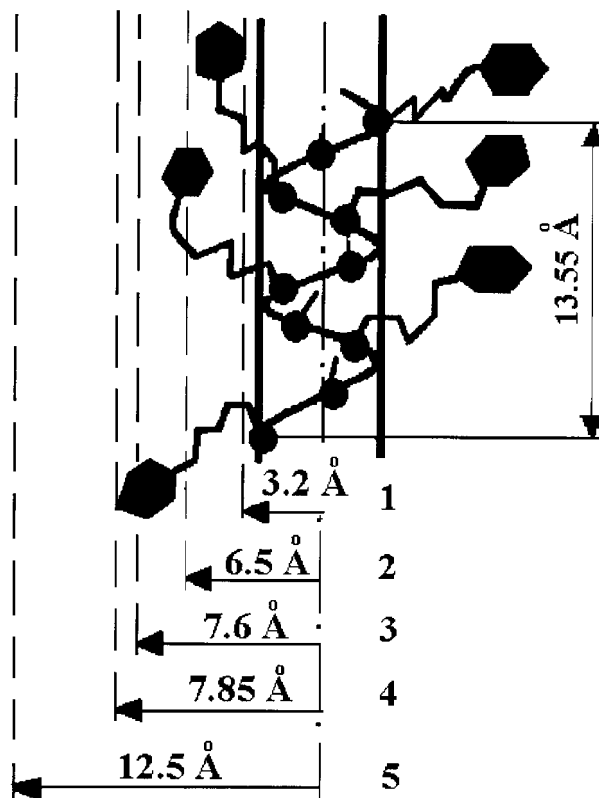


Figure 1. A comparative diagram of possible lateral dimensions of the molecular rod of PBG for calculation of the aspect ratio x , from top to bottom: 1—radius of the backbone helix plus the first side bond length^[46]; 2—half of the minimum intermolecular distance in a pseudo-hexagonal crystal lattice; 3—backbone rod radius plus side chains represented as free rotators with rms dimensions^[46]; 4—half of the intermolecular distance in crystallosolvate^[47,63]; 5—backbone rod radius plus full extended side chains.^[46]

pitch changes its sign at the so-called inversion temperature; at this temperature the pitch become infinitely high (cholesteric state transforms into nematic one) and then the pitch value decreases and the nematic LC transforms again to the cholesteric one but with the opposite sign of the screw of the cholesteric helix.^[33,34]

According to Zimmel et al.,^[46] $D = 25 \text{ \AA}$ for the side chains having a completely extended *trans* conformation. The side chains considered as independent rotators are characterized by a root-mean-square radial size of $D = 15.2 \text{ \AA}$. In a “dry” PBG at room temperature the molecules tend to pack in a quasi-hexagonal crystal lattice with parameters in the base plane of the unit cell of $a = 15.88 \text{ \AA}$, $b = 13.00 \text{ \AA}$, $\gamma = 113.7^\circ$, while heating up to 95°C leads to a hexagonal lattice with $a = b = 15.4 \text{ \AA}$, $\gamma = 120^\circ$.^[49] The intermolecular distances in the lattice of the so-called “complex phase” or in a crystallosolvate amount to 15.7 \AA (see the text below).

According to data reported by various authors, the density of PBG in the solid state varies from 1.177 to 1.280 g/cm³,^[50–52] while the crystal lattice density calculated from the x-ray diffraction data is 1.305 g/cm³^[52] or 1.320 g/cm³.^[53]

PDs of the PBG-solvent systems were most frequently studied using DMF as the solvent (Refs.^[18,22,30,46,54–64], etc.). This solvent is distinguished, among the other media, featuring the helix conformation of PBG molecules and allowing their liquid crystals to be studied in a convenient temperature interval (232–426 K), by suppressing the aggregation of PBG molecules.^[43,65] Otherwise, the aggregation could change the x value and, accordingly, modify the shape of the PD and the properties of the system under consideration.

3. SHORT REVIEW OF THE THEORETICAL PHASE DIAGRAMS OF THE SOLUTIONS OF RODLIKE PARTICLES

We will only briefly outline the history of developments that are required for the main aim of this paper. In 1949 Onsager^[25] studied the athermal ($\chi = 0$) solutions of monodisperse rodlike particles under the condition $L \gg D$ (i.e., for x tending to infinity). His analysis took into account only the steric interactions between the rodlike particles and employed a virial expansion of the free energy of the system into a series, with all the virial coefficient above the second one assumed to be zero (which is valid only for a sufficiently low solution concentration, $V_2 \ll 1$). The Onsager theory predicted the values of the first (V_2') and second (V_2'') critical concentrations of rodlike particles as functions of the parameter x , where V_2' is the minimum volume fraction of particles at which an LC phase appears in the system, and V_2'' is the minimum fraction of these particles at which the entire volume of the system is occupied by the LC phase.

Table 1. The main particulars of Onsager and Flory theories for LC state of rodlike molecules solutions (in accordance with Ref.^[67]).

Onsager ^[25] $V_2' = 3.4/x, V_2'' = 4.5/x$	Flory ^[27,28] $V_2' = 8.0/x, V_2'' = 12.5/x$
Advantages	
1. Continous medium	1. Consideration of various values of χ , of different concentration V_2 and values of $x \geq 6.4$
2. Asymptotically exact solutions at $L \gg D$ and $V_2 \ll 1$	2. A possibility of construction of a phase diagram
Disadvantages	
Consideration restricted by condition $L \gg D, V_2 \ll 1, \chi = 0$	Consideration of discrete medium (lattice model) with an artificial dividing of rodlike particles

Phase Diagram for System of PBG/DMF

7

Flory^[27,28] used a lattice model to describe a system of cylindrical particles, having length L and diameter D , surrounded by spherical particles of solvent having the same diameter D . The theory was applied to non-athermal solutions ($\chi \neq 0$) of molecules with various aspect ratios in the range $x \geq 6.4$ (according to Flory, in this range an LC phase will always form provided a sufficiently high concentration of cylindrical particles).

In Table 1 are summed the main advantages and disadvantages of the Onsager and Flory theories and expressions are given for the calculation of the critical concentrations. One must also note the work of Ishihara,^[26] which appeared at the same period of time and was devoted to an athermal solution of rodlike particles; the result $V_2' = 3.4/x$ agrees with the Onsager theory. The reasons for the quantitative discrepancies of the Onsager and Flory theories were analyzed by Khokhlov^[66] and Birshtein et al.^[67]

Khokhlov^[68-71] applied the Onsager approach to analysis of the solutions of rodlike particles, successfully eliminating the main restrictions involved in the Onsager theory. Then, as Flory, he theoretically constructed a PD of the model system. Figure 2 shows schematic PDs, based on the theories of Flory and Onsager–Khokhlov, for the case of relatively large x values. The two types of diagrams are qualitatively similar, comprising an area of isotropic phase (I), a narrow corridor of the two-phase states reflecting coexistence of the isotropic and LC phases (I + LC) at negative and small positive χ values, a broad two-phase region (I + LC) corresponding to positive χ values, a region of homogeneous liquid–crystalline state (LC), and a region of the coexistence of two LC phases ($LC_1 + LC_2$) with different ratios of polymer and solvent.

It should be noted that the theoretical calculations for large x values (see e.g., curve 1, Fig. 2a) give equal temperatures T_1 and T_2 at which the left- and right-hand walls of the two-phase corridor originate; the walls are virtually vertical. The triple point D (Fig. 2) represents a coexistence of three phases, the two LC phases and the isotropic phase. As the x value increases, the corridor narrows and shifts toward lower concentrations (cf. curves 1 and 2 in Fig. 2a).

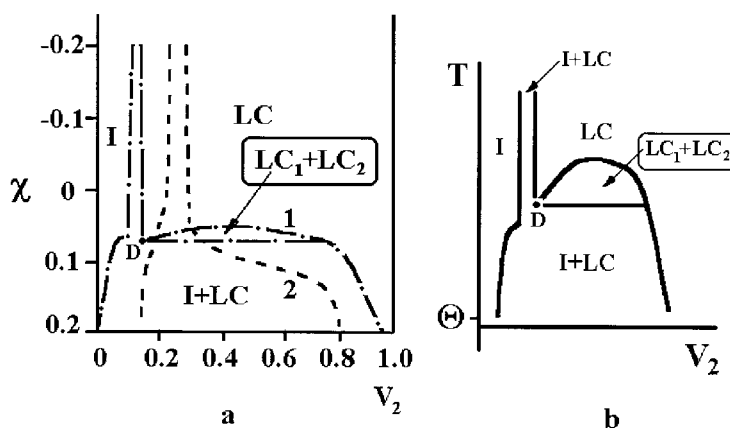


Figure 2. Theoretical phases diagrams calculated according to a—the Flory theory for $x = 100$ (1), and 50 (2)^[72,73]; b—the Onsager–Khokhlov theory^[66] for $x \gg 1$.

There have been several works devoted to a topological analysis of the PDs for the solutions of rigid rodlike molecules, considering this diagram as a combination of various types of independent phase equilibria. This approach was inspired, on the one hand, by an implicit attempt to introduce the Flory phase diagram (that did not conform to the known PD^[1,3,72]) into the PD classification of binary systems, and, on the other hand, by the necessity to take into account the properties of real polymeric systems (such as their ability to form crystals, crystallosolvates, thermotropic LC phase, to respond to the introduction of a third component, etc.^[1,3,72-76])

The first analysis of this kind was attempted by Papkov in the work,^[75] though he analyzed a particular problem of “combination and superposition of phase equilibria in polymer solutions” earlier.^[5] Analyzing the various types of PDs for polymers and low molecular weight thermotropic liquid crystals, he formulated a promising hypothesis concerning the shape of the Flory PD. It was assumed that this PD must be a part of a more complete PD describing the dilution of a thermotropic liquid crystal by an isotropic liquid. According to the hypothesis, the narrow two-phase corridor must exhibit a “bending” at high temperatures toward the pure polymer, thus restricting the region of LC solutions, and terminate at a point of transition of the thermotropic LC polymer into an isotropic melt (Fig. 3).

This hypothesis was theoretically confirmed in Refs.^[77,78], where a system of rigid rods featuring anisotropic dispersal interaction was placed into a diluent with $x = 1$. For this binary system a distinct “bending” of the two-phase corridor toward the high concentration of rigid rods^[77] was first shown, and then it was shown how the Flory diagram can be a part of a more general Papkov diagram (Fig. 4).^[78]

Papkov believed that the real PD of a two-component system always comprises a superposition of curves due to various phase equilibria including the potentially

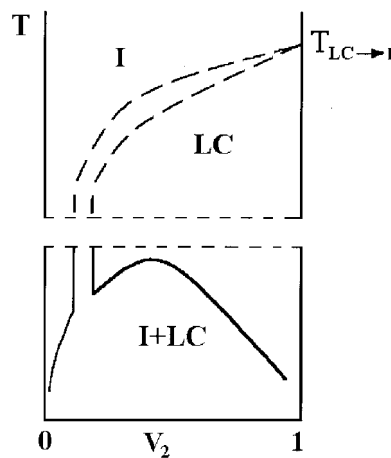


Figure 3. Hypothetical scheme of the phase diagram (in accordance with Ref.^[75]) explaining the existence of the narrow biphasic region in real system. I—*isotropic liquid phase*; LC—*liquid-crystalline phase*; $T_{LC \rightarrow I}$ —*transition temperature for the thermotropic LC phase into isotropic liquid phase*.

the components belong to the class of thermotropic liquid crystals. The liquid–crystalline polymer solutions should be classified as thermotropic liquid crystals diluted with an isotropic solvent.

A similar point of view was formulated by Ciferry.^[79] (It will be shown below that this formulation is confirmed experimentally.) A superposition of the Flory's PD, obtained for a solution of monodisperse rods, and the calculated curves of solubility of a crystalline polymer upon transition to an isotropic or anisotropic solutions was considered in Ref.^[73] (Fig. 4b). A difference between the latter curves leads to both quantitative and qualitative changes in the PD. In particular, the temperatures T_1 and T_2 at the base of the narrow two-phase corridor prove to be markedly different, which gives rise to a region of metastable states. It was also demonstrated, in the same work, that the shape of the theoretical PD may significantly depend on the choice of the interaction parameter χ . For example, in a poor solvent, the melting curve of the anisotropic phase in the region of low concentrations V_2 may increase rather than decrease with the temperature.

Papkov^[3,76,80,81] has also considered, from the general physico-chemical points of view, some combinations of various phase equilibria whereby crystallosolvate (CS) may form in the system in addition to the LC phases (Fig. 5). In this case, an LC + CS region appears in the phase diagram instead of the region representing two coexisting LC phases, and a mixture I + CS replaces I + LC in the broad two-phase region. However, these suggestions were not confirmed experimentally.

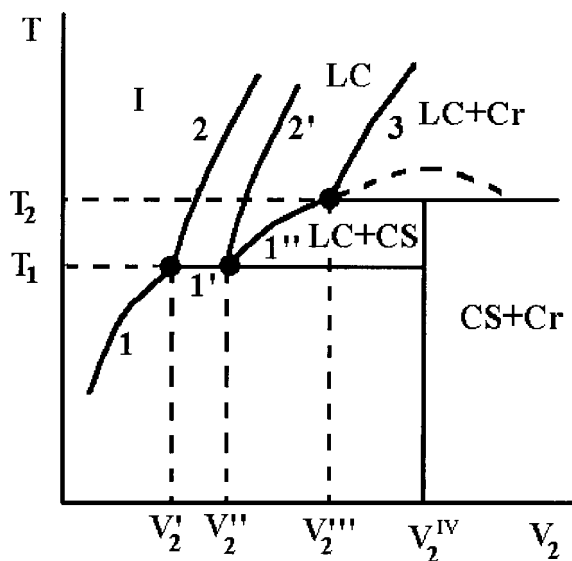


Figure 5. Hypothetical phase diagram of a solution of rodlike macromolecules with an allowance for the crystallosolvate (CS) formation.^[3,80] More detailed consideration of this type of PD will be given in the following sections.

4. EXPERIMENTAL STUDIES OF PBG-SOLVENT SYSTEMS

4.1. Concentration-Dependent Phase Transition from Isotropic Liquid to Liquid Crystal

The concentration-dependent phase transition from isotropic liquid to LC phase was most extensively studied because the critical concentrations in this systems can be rather simply determined by the method of polarized light microscopy and compared to the theoretical values.

The most simple is the determination of the first critical concentration V_2' by the observation with polarized light microscopy the appearing of the birefringence phase with an increase in PBG concentration in the solution (see, e.g., Refs.^[21,22]). Other methods were used as well, in particular the sharp change of the solution viscosity.^[82]

Slightly more complicated is the determination of the second critical concentration V_2'' . By visual or light microscopy observation of high concentration solutions some anisotropic domains located in the different layers along the view direction can be superimposed and overlap the entire field of view; thus, the illusion can be produced that the entire volume is occupied by an anisotropic phase. The concentration at which the boundary between the isotropic and anisotropic phases reaches the meniscus sometimes can be taken as $V_2''^{[64]}$ although the thus determined values of V_2'' , of course, will be underestimated.

Figure 6a shows a scheme for another kind of the V_2'' determination by visual or light microscope technique^[83]: one plots the volume fraction of the isotropic phase V_1 as a function of the volume fraction V_2 of polymer in solution; at first we will have $V_1 = 1$, but then, starting from V_2' , the value of V_1 must decrease linearly. At high values of V_2 some deviations from linearity can be observed, the value of V_2'' can be determined by the extrapolation of V_1 to zero.

Recalculation of the weight concentrations as volume concentrations can be produced by the formula:

$$V_2^{\text{vol}} = V_2^{\text{sp}} / [V_2^{\text{sp}} + (1 - V_2^{\text{wt}})V_1^{\text{sp}}/V_2^{\text{wt}}] \quad (1)$$

where V_2^{vol} and V_2^{wt} are the volume and weight polymer fractions in the solution; the specific volumes of solvent and polymer can be taken as $V_1^{\text{sp}} = 1.058 \text{ cm}^3/\text{g}$ and $V_2^{\text{sp}} = 0.786 \text{ cm}^3/\text{g}$, respectively. Note that the passage from volume to weight fractions of a polymer in solution does not qualitatively modify the PD as a whole and does not change the shape of the concentration dependencies of various parameters of the system. Obviously this is due to the linear relation between V_2^{wt} and V_2^{vol} in the most interesting interval from 0.2 to 0.7 (Fig. 6b). In particular, for the determination of V_2'' (see Fig. 6a) it is possible to plot V_1 versus weight fraction of polymer. In Ref.^[84] an IR-spectroscopy method was used for the determination of the V_2'' value. Note that unless otherwise indicated, the concentrations below are given in the units of wt.%.

Figure 7a shows a comparative representation of theoretical and experimental values V_2' , obtained by various authors^[57,58,64,82,85,86] and gathered by Flory in his review.^[87] For calculations of the aspect ratio the formula $x = MI/M_0D$ was used, where D is the diameter

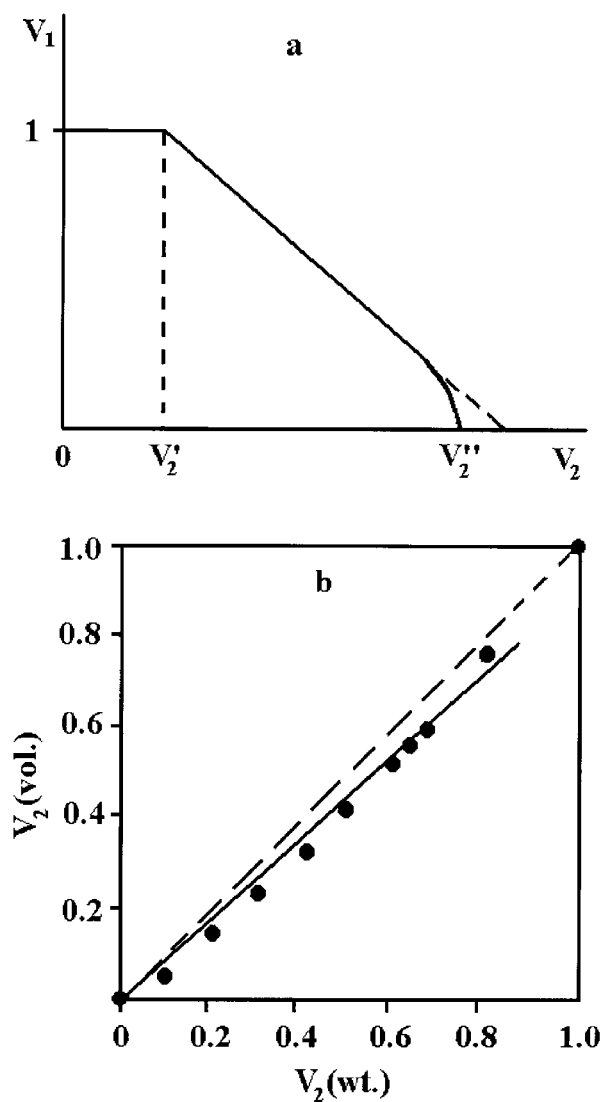


Figure 6. Scheme of the determination of the second critical concentration V_2'' (a) and the relationship between the volume and weight concentrations of PBG in DMF solutions (b).

of the molecule, M is its molecular mass, $M_0 = 219$ is the mass of the repeat unit, and $l = 1.5 \text{ \AA}$ is the length of the repeat unit projection on the molecular helix axis.

The agreement of calculated and experimental data is satisfactory especially if one takes into account that in the mentioned works samples of PBG with a relatively high molecular mass from 2.2×10^5 to 3.4×10^5 were used. Such molecular masses are comparable, or some exceed, the molecular mass $M = (1.5 - 2.0) \times 10^5$ corresponding to the persistence length of PBG molecules ($\sim 700 - 1600 \text{ \AA}$) in α -helix

Phase Diagram for System of PBG/DMF

13

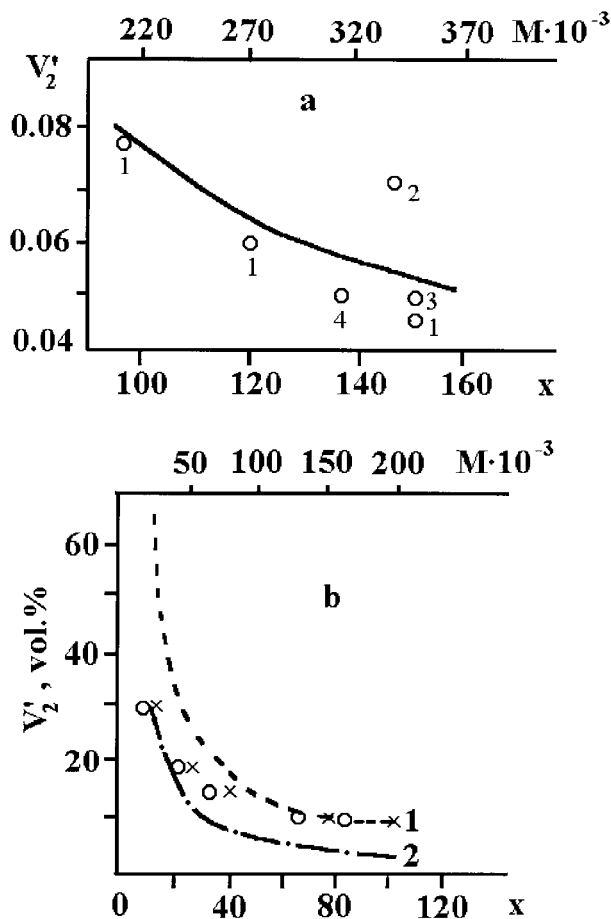


Figure 7. The plots of the first critical concentrations versus aspect ratio or molecular mass of PBG: (a) calculation based on the Flory theory (solid line) and the experimental data (points) for the PBG solutions in various solvents: m-cresol (1)^[82] and (2)^[85], DMF with the additives of methyl alcohol (3)^[86] and (4)^[57,58]; (b) calculations based on the Flory (1) and Onsager theory (2) (lines) and the experimental data for the PBG solutions in DMF (points).^[64]

conformation^[88–93]; strictly speaking, this factor does not allow modeling the molecule by an absolutely rigid rod.

In Ref.^[62] solutions of PBG (with M from 2.6×10^4 to 2.0×10^5) in DMF were investigated; the experimental values of V_2' were compared with the calculated ones on the basis of different theories (Fig. 7b). The Onsager theory shows a better agreement at low molecular masses of polymer, while the Flory theory provides a better description at high molecular masses. Similar conclusions were made in Ref.^[94]. In general it can be concluded that both types of theories give values of the critical concentrations that qualitatively agree with experiment. As for the quantitative results, the experimental critical concentrations fall between the values calculated by the two theories.

Let us consider the data available on the critical concentrations at various temperatures (i.e., on the entire two-phase corridor). Figure 8 shows the first experimental PD of the PBG solutions in DMF reported by Miller et al.^[54–60] Although the authors believed that their experiments generally confirmed the Flory theory, the published data also revealed the main discrepancies between the earlier theory and experiment. One of these features consists in the above-mentioned “bending” of the two-phase corridor toward higher concentrations with increasing temperature.^[54] Besides the “bending,” the data of Miller et al.^[54,57] revealed a maximum in the region of low concentrations (Fig. 8b, c);

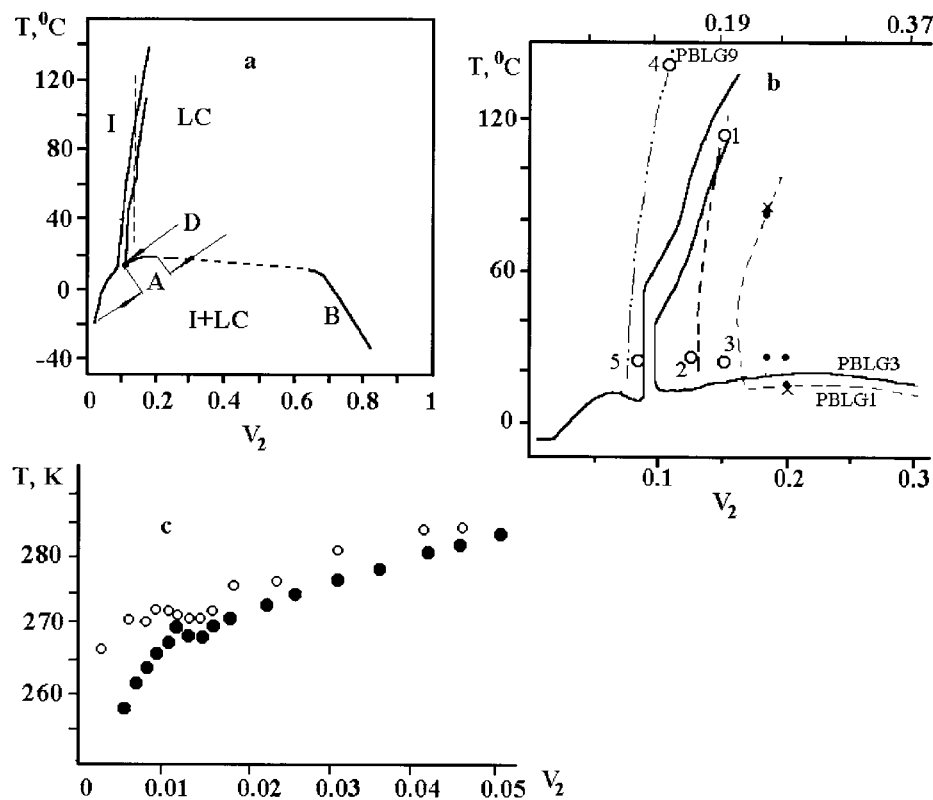


Figure 8. Phase diagrams of PBG solutions in DMF measured in the regimes of (a, b) heating and (c) cooling^[57,58,61]: (a) $M = 3 \times 10^5$; region A is plotted from NMR data,^[54,102] region B is obtained by an isopiestic technique,^[59] D is the triple point, the dashed vertical line corresponds to the composition studied in Ref.^[102] (see also Fig. 12); (b) effect of molecular mass on phase boundaries from Ref.^[54], various points were obtained by different methods, open circles—by polarizing microscope, filled circles and crosses—by NMR technique. The solid lines show a part of the phase diagram for the same PBG as in Fig. 8a ($M = 3 \times 10^5$), the dashed lines show a part of the phase diagram for PBG with $M = 1.2 \times 10^5$, and the dashed-dotted line shows only the left branch of the corridor for PBG with $M = 9 \times 10^5$; (c) a part of the phase diagram in the region of small PBG concentrations constructed by visual observation of the process of gel formation (open and black circles representing the start and end of the gel formation, resp.).^[57]

Phase Diagram for System of PBG/DMF

15

the results, plotted in Fig. 8b and 8c, were obtained by heating and cooling, respectively. The data in Fig. 8c were obtained by the visual observation of gelation. The upper curve corresponds to the beginning of this process and the lower to its finish.

Miller^[55,57,58] believed that the “bending” reflects an increase in the flexibility of the molecular rods with temperature. As was mentioned above, in order to explain this feature, Papkov developed a concept of the thermotropic origin of the LC solutions of rodlike molecules^[1,76,75] by considering the real PD as a superposition of various curves of phase equilibria.^[75] From this standpoint, the “bending” of the two-phase corridor, its narrowing, and the crossing of two branches at the melting point of pure PBG from the state of thermotropic liquid crystal to an isotropic liquid appears to be quite natural. However, because this melting point falls within the region of thermal degradation of many rigid-chain polymers it was considered that experimental verification of the hypothesis is hardly possible. As we will see, this is not so for PBG solutions. Ciferry^[79] explained the experimental “bending” on the basis of the Warner-Flory theory^[77] and also believed that one of the components of an LC rigid chain–solvent system must occur in a thermotropic LC state.

Similar “bending” was observed for the poly- ϵ -carboboxy-L-lysine solutions in DMF^[56,57,59] and for the poly-p-phenylene-terephthalamide solutions in sulfuric acid.^[95,96] The bending was also found for solutions of PBG of different molecular masses.^[97]

Figure 9 shows the parts of the PD of the PBG-DMF system obtained by visual determination of the turbidity points and thermo-optical measurements.^[98] These data also

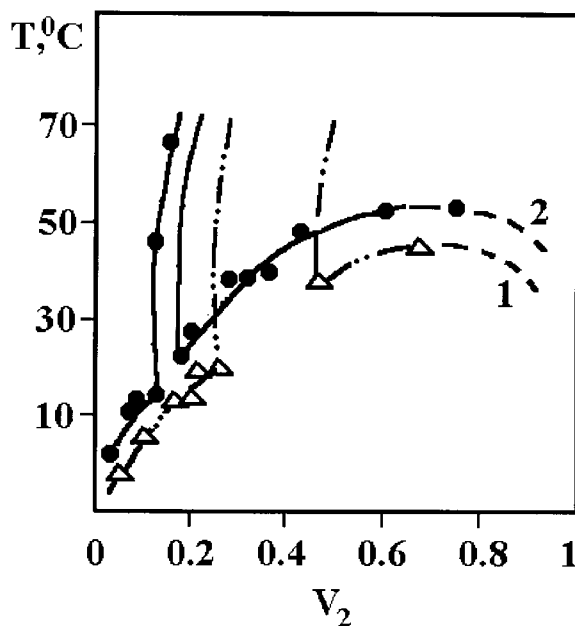


Figure 9. Parts of the phase diagrams of PBG solutions in DMF^[98]; $M = 5 \times 10^4$ (1) and 2×10^5 (2).

revealed “bending” of the corridor and a clear difference of the T_1 and T_2 temperatures corresponding to beginnings of the left- and right-hand walls of the corridor. At first sight the difference of the T_1 and T_2 values confirms the notions of Papkov^[3,74,76] and Balbi^[73] on the superposition of various types of phase equilibria but, as will be shown in this case the situation is more complicated. However, the combination of the phase equilibria of various types leads to fundamental differences of the experimental PDs from the theoretical PDs of Flory and Onsager—Khokhlov, taking into account only a single type of phase equilibrium (isotropic liquid—LC).

Volchek et al.^[97,99] studied the temperature dependencies of the critical concentrations of PBG in DMF solutions (Fig. 10). They observed the increase in critical concentrations (or the corridor “bending”) with temperature but explained it by the disruption of aggregates of PBG molecules during the heating. In the model experiments the authors added to the solutions small quantities of trifluoroacetic acid and considered that it also disrupts the aggregates. In agreement with their idea they obtained in the latter case an independence of critical concentrations on the temperature and correspondingly the absence of the corridor “bending.”

If one considers the author’s conclusion to be valid then it must be related only to the investigated and very restricted temperature interval. However, the “bending” must exist, because a temperature of disordering of the LC monophasic (i.e., its transition into isotropic state) must exist also. Thus, a disruption of polymer aggregates during heating can explain the temperature independence or weak temperature dependence of critical concentrations only in a restricted temperature interval. Besides, in our opinion, the small additions of trifluoroacetic acid to the PBG solutions can disrupt not only the aggregates but also some intramolecular H-bonds at local points of the PBG α -helix that leads to a decrease in the rigidity of molecular rod and therefore a decrease in its aspect ratio and corresponding increase in critical concentrations.

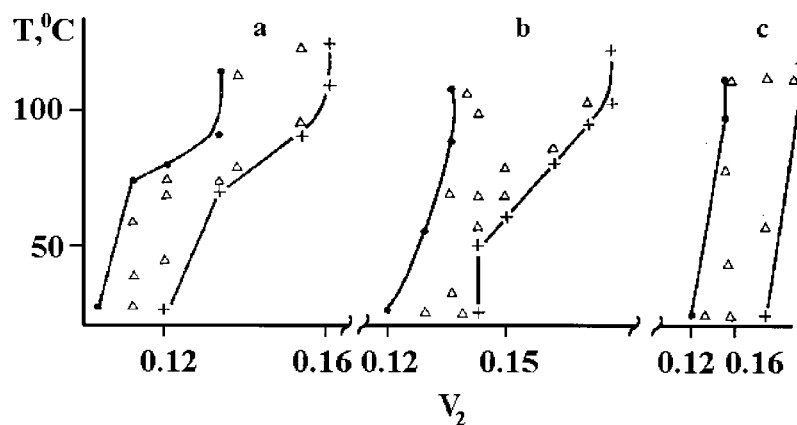


Figure 10. Phase diagrams of different molecular masses PBG solutions in DMF: $M = 3 \times 10^5$ (a), 2×10^5 (b), and 1.2×10^5 (c).^[97]

4.2. Effect of Molecular Mass on the Shape and Position of the Narrow Biphase Region

Effects of the molecular mass of a polymer, that is, of parameter x , on the shape of the PD were first studied in Ref.^[22], and then in a number of works (e.g. Refs.^[54,82,84,86,98,99]). In particular, Miller showed^[54] that an increase in the molecular mass shifts the narrow two-phase corridor to lower concentrations (see Fig. 9b). Based on his experimental data Miller^[54,55] concluded that the PD changes upon variation of the molecular mass in complete agreement with the Flory and Ronca theory.^[28,100,101] However, this conclusion is not quite correct, because the theory cannot account for a major part of the phase diagram and only describes, to a certain approximation, the narrow two-phase corridor.

The influence of molecular mass was investigated also in Ref.^[98] (see Fig. 10). If, as according to Refs.^[73,74], the parts OA and BC of the experimental PD in Fig. 9 are considered as the curves of the solubility in isotropic and anisotropic solvent respectively, then it follows from this figure that an increase in PBG molecular mass reduces the solubility (for higher molecular mass the curves OA and BC occur at a higher level) or, what is the same, reduce the polymer-solvent interaction. In agreement with this factor the T_1 and T_2 shift to lower temperatures with an increase in molecular mass. Besides, it is seen that the corridor width reduces with increasing in the molecular mass.

Nakajima et al.^[86] studied the PD of a ternary system PBG-DMF-methanol, in which the addition of methanol increase the values of V_2' . The PDs for these systems were obtained at a constant temperature and different values of x (150 and 350). In accordance with all main theories, the increase in x led to narrowing of the two-phase corridor and its shift toward lower concentrations.

Thus, from the experimental data it can be concluded that an increase in the molecular mass (or x) of the polymer leads to (1) a shift of the corridor base to smaller concentrations; (2) a narrowing of the corridor; and (3) a shift of the corridor to lower temperatures.

4.3. Character of the Transition from the LC Phase into a Broad Two-Phase Region (Miller's Studies)

In accord with the theory, a transition from LC to a broad two-phase region in solutions of rodlike molecules may be accompanied by separation of the system into two LC phases having different polymer concentrations (see Fig. 2). Special efforts to detect this transition and determine the region of coexistence of the two LC phases were devoted in the works of Miller et al.,^[57-59] where an attempt was made to construct the PD in the entire range of PBG concentrations (Fig. 8a). The dashed line in Fig. 8a shows the part of the PD not determined in that work. However, the authors believed that connection of the two experimentally measured parts (A and B) implies convexity of the missing part of the phase curve from the side of high temperatures, thus providing for the existence of a region where two LC phases may coexist.

Portion A of the PD in Fig. 8a was obtained by NMR,^[54] while portion B was determined by the isopiestic method.^[59] Both techniques are not direct methods for the detection of phase transitions. However, taking into account that portion A agrees

qualitatively with the published results obtained by different methods, these data are undoubtedly reliable. At the same time, the character of portion B contradicts the DSC data of some other researchers.^[18,61,62]

Russo and Miller^[102] undertook special experiments in order to refine the behavior of the phase curve in the vicinity of portion A. The study was performed by measuring the temperature dependence of the cholesteric helix pitch by the method of small-angle scattering of linear polarized light. The idea and the scheme of experiments are illustrated by Fig. 11a–d. They measured the pitch value, P , of the cholesteric structure in a 12.87% PBG solution in DMF during cooling from 100° to 14°C (the dashed lines in Fig. 11a, c) to reach the phase equilibrium curve (point C in the figure). Before the reaching of point C, the value of P will decrease in accordance with the temperature dependence of P in the given solvent. However, after the moment when the system reaches the phase curve the type of change of P depends on the shape of the PD. If the PD has the shape, presented in Fig. 11a, then after achievement of the point C in the phase curve the system will decompose into two LC phases. In this case most of the system will be occupied by the dilute LC phase (the volume of which is determined by the known “lever rule”) with an increase in P during further dilution, determined by a decrease in the temperature.

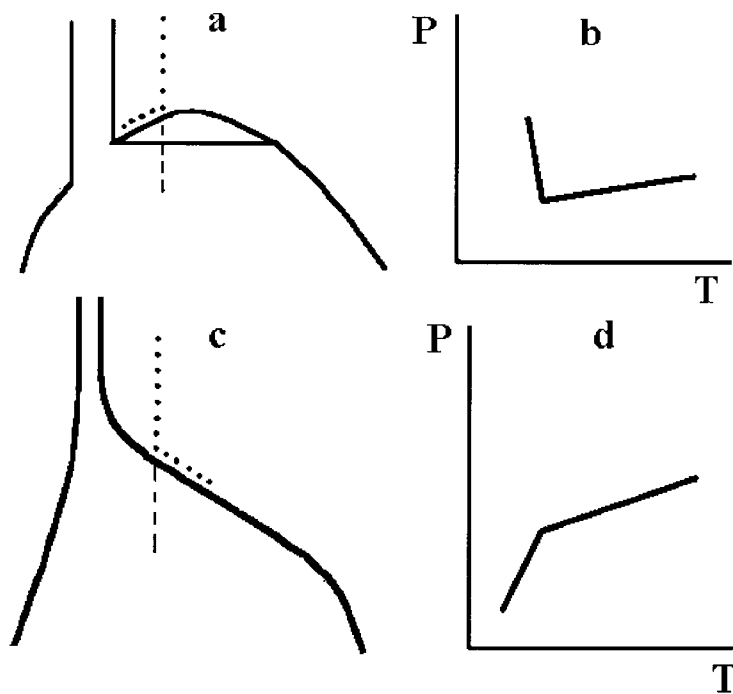


Figure 11. Scheme for clarifying the idea of Miller's et al.^[102] experiments for the confirmation of the existence of two LC phase regions in the phase diagram of PBG-DMF system: (a) hypothetical scheme of the phase diagram with a ($LC_1 + LC_2$) region and (b) corresponding temperature dependence of the cholesteric pitch; (c) hypothetical scheme of the phase diagram without a ($LC_1 + LC_2$) region and (d) corresponding temperature dependence of the cholesteric pitch.

Phase Diagram for System of PBG/DMF

19

An effect of a relatively small amount of concentrated phase on the observed P value can be neglected. The plot of $P(T)$ must have the shape presented in Fig. 11b. In the opposite case, if the PD has a shape as in Fig. 11c, after the achievement of the phase curve the system will decompose into an isotropic solution and concentrated LC phase, and therefore the P value will decrease again but more sharply, as shown in Fig. 11d, because the concentration of the LC phase will increase. The experimental plot of $P(T)$ agrees with Fig. 11b. Therefore, the authors made the conclusion that a region of two LC phases on the PD exists.

In our opinion, however, these data only proved that the phase equilibrium curve exhibits an increase with the temperature in the concentration range studied, and that the system separates into two phases, one of which is a dilute LC phase. As for the nature of the second phase and the behavior of the phase equilibrium curve during further growth of the concentration, these questions remained open and will be considered below.

4.4. “Complex” Phase

Luzzati et al.^[103] studied the PBG-DMF system by an x-ray diffraction technique and showed that a broad two-phase region observed at $V_2 = 15-70\%$ and room temperature contains a “complex” phase characterized by a special system of reflections differing from reflections corresponding to the crystal phase of a dry polymer. The positions of the reflections did not change as the concentration varied within the limits indicated above. This implies that the composition of the “complex” phase (containing a certain amount of solvent) also remained unchanged.

Detailed study of the “complex” phase structure was carried out at $V_2 = 55\%$ in Refs.^[47,104] It was shown,^[47] that the benzene rings of the PBG side chains in the “complex” phase have a quasi-helix order, differing from the α -helix periodicity of the main chain, and form stacks. The stacks of neighboring chains unite into one continuous quasi-helix configuration of side chains.

In further investigations it was shown that the “complex” phase has a hexagonal lattice and four chain pass through the unit cell.^[61] However the content of the solvent in the “complex” phase was determined only in Ref.^[63] (see Section 4.6).

4.5. Gelation

The passages from an isotropic state, a two-phase corridor, or an LC state to the broad two-phase region in the systems of PBG and a helix-forming solvent were always accompanied by gel formation.^[18,54,57,58,98,105,106] Gelation has been observed even at concentrations as small as 0.03–0.05%.^[18,58] Miller et al.^[56] explained the gel formation by special features of the spinodal decay kinetics and believed that these gels are nonequilibrium thermodynamically. By electron microscopy they demonstrated that the gels comprise a network formed by bundles of the macromolecules with a diameter from several hundreds to about a thousand Angströms, typically spaced by approximately 1 μm .

A similar gel structure was described by Uematsu and Uematsu (Fig. 12),^[18] however, they considered that the network nodes consisted of the “complex” phase.

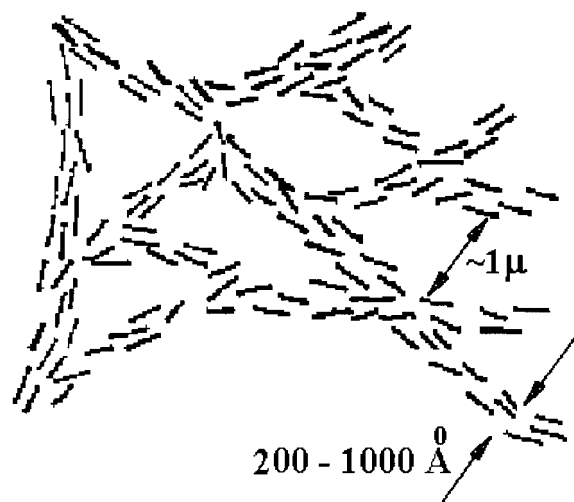


Figure 12. Model of the structure of gels (networks) formed by the aggregation of rigid rodlike molecules. This model was proposed on the basis of electron microscopy data for gels obtained from very dilute (0.5%) PBG solutions.^[18]

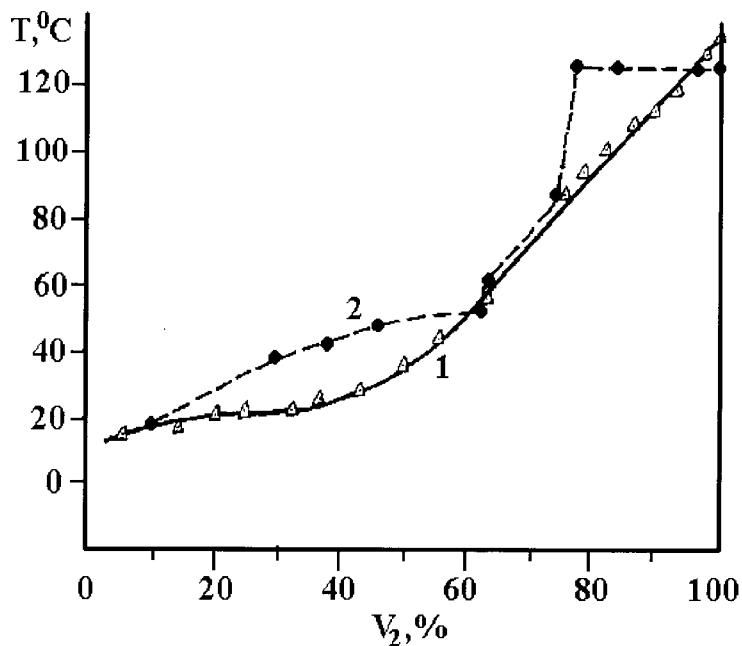


Figure 13. The plot of transitions temperatures versus concentration determined for PBG-DMF systems by DSC: 1—Ref.^[18]; 2—Ref.^[64].

Phase Diagram for System of PBG/DMF

21

At a PBG concentration below 20% they could not find x-ray reflections of the “complex” phase, but nevertheless, Uematsu et al.^[18] believed that the “complex” phase was present even in the gels formed in systems with low PBG concentrations, suggesting that this was confirmed by a continuous concentration dependence of the gel melting temperature determined by DSC (Fig. 13, curve 1).^[18,61]

A sharp variation in the properties of gels was observed at a polymer concentration of approximately 60%.^[18,61] For this reason, the transition temperatures were not determined in the concentration range from ~58% to ~72% (see Fig. 13, curve 1). At a higher concentration, the peaks in the thermograms broadened and the transition became irreversible. The melting of the gels was classified into three groups, depending on the initial solution concentration.^[18] The melting of dilute gels (<18%) leads to the formation of an isotropic phase, while the melting of moderately concentrated gels (20–60%) is accompanied by a transition of a mixture of the “complex” phase and a solvent-rich phase into a LC phase. The “complex” phase contains a stacked structure of benzene rings of the side chains. The melting of gels with a still higher concentration (>70%) leads to collapse of the stacked structure.

Similar DSC data were obtained in Ref.^{[64]a}. Figure 14 shows these DSC curves for the PBG solutions of various concentrations. As the polymer concentration increases, the intensity of endothermic peaks corresponding to the gel melting initially grows, and the peaks shift toward higher temperatures. At a concentration of approximately 63%, the character of the DSC curves changes: a high-temperature shoulder appears, grows, and shifts to higher temperature (Fig. 14, curve 4 and Fig. 14b, curve 1), while the “main” peak broadens so as to hinder determination of the melting point (Fig. 14b, curves 2,3).

Figure 13 shows matched thermograph data compiled from both works.^[18,64] Their discrepancies apparently related to different experimental conditions and molecular masses (2×10^5 and 3.1×10^5 , respectively). The DSC data of Ref.^[64] agree well with the results obtained by using other methods for detection of the gel formation in the concentration range up to ~63%.^[98] Therefore, in the further construction of the corresponding curve of phase equilibrium in this concentration range, preference was given to the data of Ref.^[64]. In the region of high PBG concentrations in DMF, where a “complex” phase and crystallites are formed, the data of Refs.^[18,61] were preferred because the cells used in Ref.^[64] were not hermetically sealed sufficiently, 2 feature especially manifested at elevated temperatures.

The partial evaporation of solvent apparently led to intense crystallization.

Note, however, that good agreement of the data from both works is observed for the concentration range close to a 100% content of the “complex” phase (~67% PBG) and a 100% content of PBG. The temperatures of the transition from crystalline into LC phase at $V_2 = 100\%$ reported by the two groups of researchers,^[18,61,64,98] are rather close (130°C versus 137°C, respectively), although the difference may reflect the effect of molecular

^aWe note that in Refs.^[64–98] and other of our works PBG synthesized by the known scheme^[41,107,108] of polycondensation of corresponding N-carboxy-anhydride in benzene, with tri-ethylamine as initiator was used. This technique leads to narrow molecular mass distributions.^[109,110] The synthesis was carried out during many years for our works by a chemical laboratory headed by Prof. T. A. Sokolova and then by Prof. G. P. Vlasov. We are very grateful to them and to their colleagues.

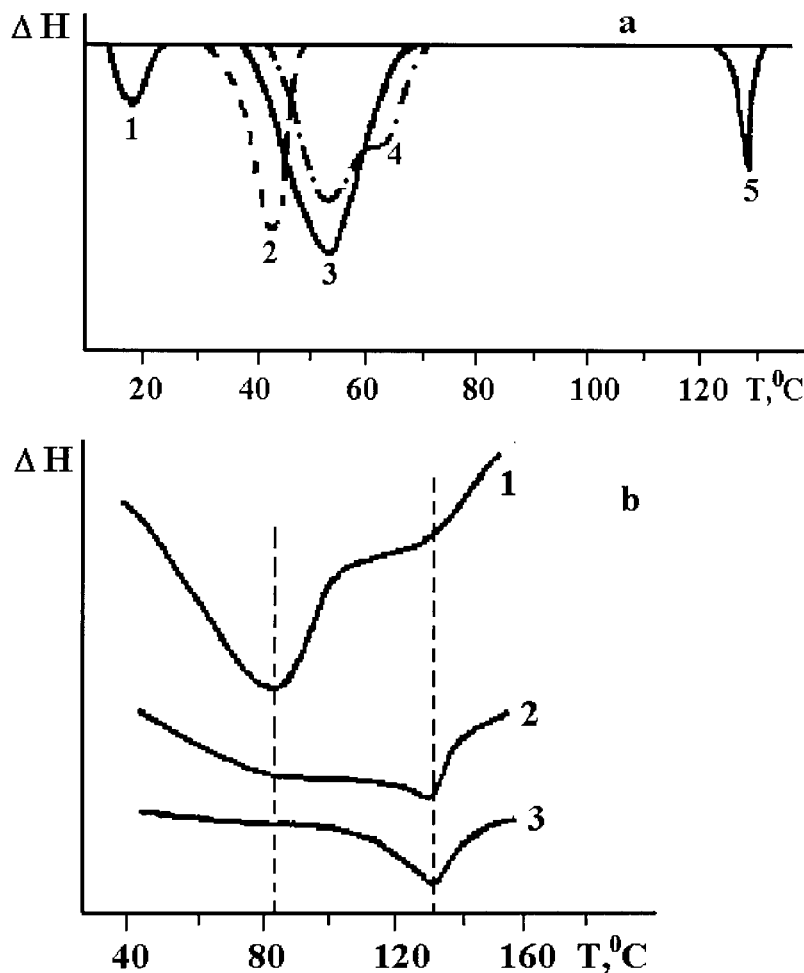


Figure 14. DSC thermograms for PBG-DMF systems at various concentrations of PBG plotted in accordance with Ref.^[64]: a—9.6 (1), 38.0 (2), 62.8 (3), 65.4 (4), and 100% (dry film, obtained from the PBG solution in DMF) (5); b—76.4 (1), 82.7 (2), 96.0 (3). Molecular mass of PBG was 2×10^5 .

mass of the polymer rather than be merely a random scatter. The specific heat of the transition to the broad two-phase region (normalized to the PBG content) was 6–8 kJ/mol.^[57]

Russo and Miller^[60] explained the formation of the “complex” phase by the presence of water ($\sim 1\%$) in the PBG-DMF system. However, this factor was eliminated in Refs.^[62–64,98] where the DMF was dried over calcined zeolite and the amount of residual water, as monitored by gas chromatography, did not exceed 0.01% and could be ignored according to Ref.^[60]. Nevertheless, the formation of the “complex” phase was unambiguously detected under the anhydrous conditions.^[64,98]

Phase Diagram for System of PBG/DMF

23

Figure 15 shows a part of the PD of the PBG-DMF system for PBG with a molecular mass of $M = 2 \times 10^5$.^[64] This part of the PD was determined by five different techniques. In particular the points on the curve of phase equilibrium were determined taking into account the fact that, as noted above, the transition to a broad two-phase region is always accompanied by gel formation. The temperatures of gel formation were determined by the two rheological techniques.^[64] During the measurements, the gel was heated with a rate 0.2° per 30 min. The temperatures of gel formation determined by these two techniques coincided to within the experimental error, about $1.5\text{--}2.0^\circ$. During cooling with the same rate the temperatures of gelation were $5\text{--}7^\circ$ less. The same difference was observed between the transition temperatures determined during heating and cooling by the visual registration of the turbidity. Figure 15 shows the results of heating.

The transitions from both the isotropic phase and the LC state led to the formation of macroscopically homogeneous gels with different structures. Note that gels of the first type (isotropic phase plus anisotropic network nodes) had only one anisotropic phase, while in the second type (LC state plus anisotropic nodes) both phases are anisotropic. Accordingly, the gels of the two types were referred to as isotropic–anisotropic or anisotropic–anisotropic.

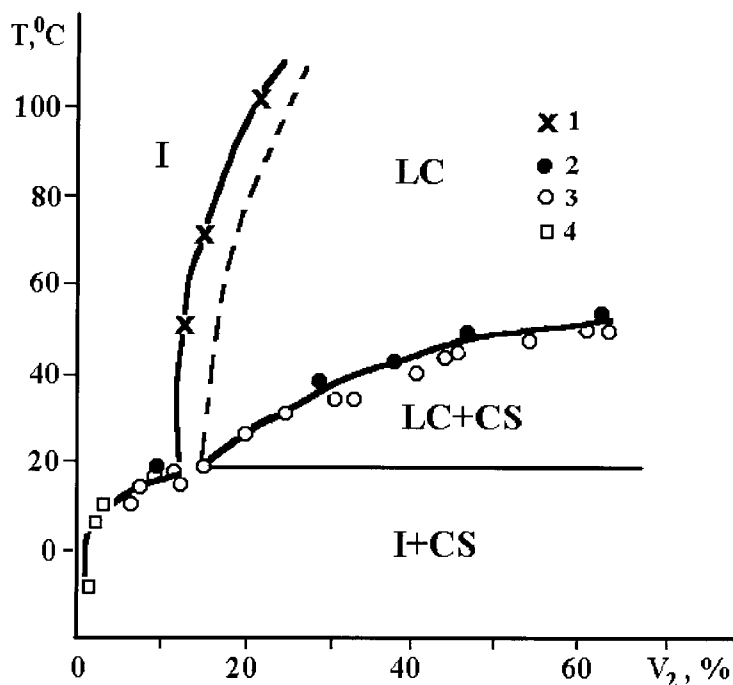


Figure 15. A part of phase diagram of the PBG-DMF system determined by various method (in accordance with Ref.^[64]): (1) optical polarization microscopy, (2) DSC, (3) visual determination of the turbidity points plus the method of weight-induced fluidity losses, and (4) elastic gel detection (“throw-ball” technique).

Interesting phenomena were observed for transitions in the systems occurring within the narrow two-phase corridor of a sufficiently large width (e.g., in PBG with $M = 5 \times 10^4$.^[98]) The samples were placed into sealed ampoules. At temperatures in the range $T_1 < T < T_2$ only the anisotropic part of the system, occurring in the bottom part of the ampoule, was found in the gel state, while an isotropic fluid phase was observed in the top part. It was only at $T < T_1$ that the isotropic phase also converted into a gel state. The interval $T_1 < T < T_2$ is characterized by a large probability of forming metastable gels (which will be discussed below). However, on the transition from LC to gel state the gel components exhibited the same structure irrespective of the initial solution concentration, which is indicative that the system was close to the thermodynamic equilibrium. The same is indicated by nearly equal values of the transition temperatures determined by various methods, including optical, rheological, and thermograph techniques (see Fig. 15), and by a small difference (within 5–7°C) between the values measured in the slow heating and cooling regimes. It should be noted that a change in the state of the solution is observed at concentrations above ~67%, whereby the samples convert from gel-like into nontransparent paste-like systems.^[98]

4.6. X-ray Diffraction Studies of the LC State and the Transition from the LC Phase into a Broad Biphasic Region

Robinson et al.^[22] used x-ray diffraction techniques to study the dependence of the intermolecular distance d (in the direction perpendicular to the long axes of the molecular rods) in liquid-crystalline PBG solutions in dioxane on the polymer concentration V_2 . It was found that the intermolecular distance decreases by the law $d = 127/\sqrt{V_2^{vol}}$ with increasing V_2 ; the spacing corresponds to hexagonal packing of molecular rods in solution.

A similar dependence was reported for the liquid-crystalline PBG solutions in DMF at 70°C.^[63] In the same work the authors studied the transition from the LC state to the broad two-phase region in the PBG-DMF system by the WAXS method. The experiments, unlike those reported in Refs.^[103,104], were performed on nonoriented samples. This led to a decrease in the intensity of reflections, so that only the most intense diffraction features were observed. Figures 16a, b present simplified patterns of the x-ray photographs, while Fig. 16c shows how the position of the system on the PD varies in the course of the experiment, and assigns the reflections to various points on the PD. The LC state is characterized by a strong reflection, corresponding to the spacing d_1 (Figs. 16a and 17a) between PBG molecules measured in the direction perpendicular to the molecular axes, and an amorphous halo (Fig. 16a). Upon transition to the broad two-phase region (20–22°C), the diffraction patterns showed two new reflections (Figs. 16b and 17b). This transformation of the x-ray diffraction pattern was reproduced during variation of the solution concentration within wide limits (at least from 16.6 to 63%). (At higher concentrations, the form of the diffraction pattern was strongly dependent on the method of sample preparation, sometimes showing new reflections characteristic of the crystalline PBG lattice.) The positions of the reflections obtained from the LC phase and the corresponding spacing d_1 depend on the concentration in accordance with the hexagonal

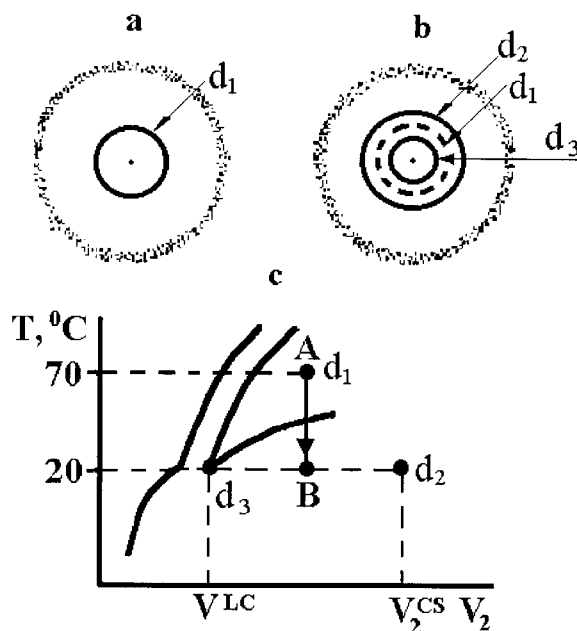


Figure 16. Schematic of x-ray diffraction patterns of (a) an unoriented monophasic LC solution and (b) a two-phase system. Schematic diagram (c) illustrates a transfer from (a) to (b): on cooling of the monophasic LC system characterized by the reflection d_1 from an elevated temperature (point A) to room temperature (point B) the system decomposes into two phases characterized by main reflections d_2 and d_3 .^[63]

model of PBG packing and in agreement with the data of Robinson et al.^[22] (Fig. 18). After cooling the sample to 20°C , the x-ray diffraction patterns retain traces of the initial reflection due to the LC state (Fig. 17b). The position of the “external” reflection, with a spacing $d_2 = 15.7 \pm 0.2 \text{ \AA}$, agrees well with that of the most intense reflection from the “complex” phase and does not change with the concentration. The “internal” reflection, corresponding to a spacing of $d_3 = 32.5 \pm 0.3 \text{ \AA}$, characterizes a more dilute LC phase formed at 20°C . At constant T the position of this reflection also remains unchanged upon variation of the polymer concentration V_2 .

Figure 19 shows the concentration dependencies of d_1 , d_2 , and d_3 . The curve of $d_1(V_2)$ (dashed line) crosses the two other plots (parallel to the abscissa axis) at a concentration of $15 \pm 1\%$ and $67 \pm 2\%$. The former value agrees well with a concentration determined from the PD for the dilute LC phase at room temperature (near the triple point), while the latter corresponds to a pure “complex” phase (see Figs. 15 and 16c). Based on the molecular masses of DMF (73 a.m.u.) and the repeating unit of PBG, (219 a.m.u.) it was concluded^[63] that the “complex” phase has three DMF molecules per two repeating units of PBG. However, a structure model with mutual positions of PBG and solvent molecules has not been proposed up to now. At concentrations exceeding $\sim 67\%$, the x-ray diffraction patterns showed new reflection characteristic of the crystalline lattice of PBG.^[64]

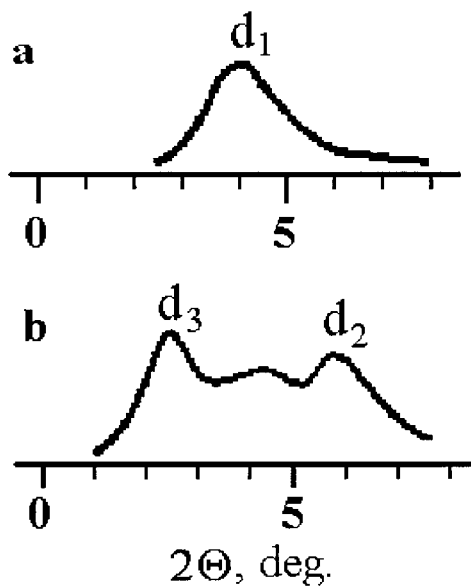


Figure 17. Some x-ray diffractograms of the systems PBG-DMF (Ni-filtered CuK_α -radiation): (a) LC solution $V_2 = 25.9\%$, 70°C ; (b) two-phase system (LC + CS) with the same concentration at 20°C .^[64]

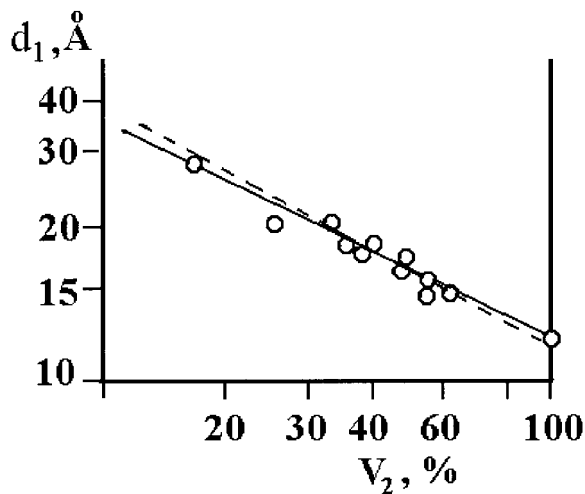


Figure 18. Logarithmic plot of the intermolecular distance d_1 versus the PBG concentration in DMF at 70°C (LC state).^[63] Dashed line corresponds to a hexagonal packing of molecules in accordance with Robinson's results.^[22] The point at $V_2 = 100\%$ correspond to the intermolecular distance in a crystal lattice.^[42,64]

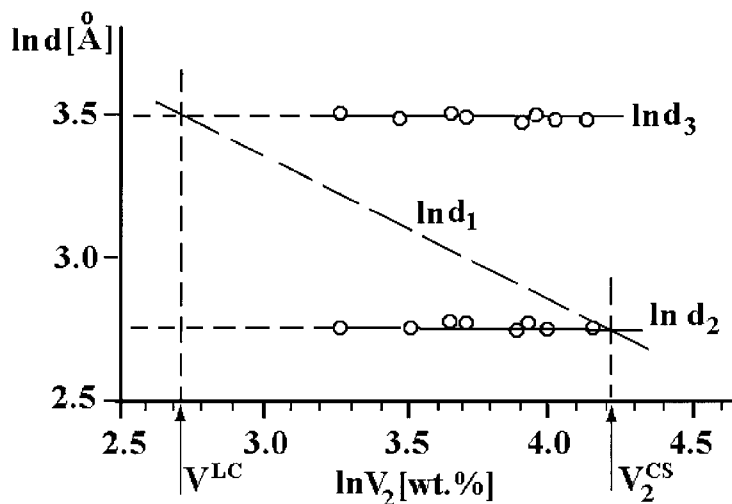


Figure 19. Plot of the interplanar spacing (1) d_1 (determined at 70°C), d_2 (20°C), and d_3 (20°C) versus the PBG concentration in DMF.^[63]

5. CONSTRUCTION OF THE FULL PHASE DIAGRAM FOR THE PBG-DMF SYSTEM

5.1. Identifying the “Complex Phase” with Crystallosolvate Phase and Its Position in the Phase Diagram

Crystallosolvates have been observed for different synthetic polymers.^[111–116] Apparently, the formation of crystallosolvates is characteristic of polymers susceptible to a specific interaction with a solvent. In Ref.^[115] crystallosolvates in a mesogenic system of rodlike polymer-solvent were found in the first time.

The experimental data considered above, which were obtained by different methods, suggest that both the behavior and properties of the PBG-DMF system sharply change upon passage through the point with a polymer concentration of approximately 63%. These changes (summed up in Table. 2) apparently are related with an appearance in the system of a sufficiently large fraction of the “complex” phase referred to as the crystallosolvates.

The molar ratio of solvent to solute in the DMF-PBG system, 3:2, is typical for the crystallosolvates: the amount of solvent, on the one hand, must not exceed the amount of structural units of dissolved substance (in our case, the number of repeat units of PBG) and, on the other hand, must not be too low (at least, not below a minimum level necessary to form the first solvent envelop around the polymer molecules).

Moreover, the presence of crystallosolvates identified with the “complex” phase explains the change in properties of the system observed upon crossing the corresponding concentration threshold, and the thermoreversible gel formation (see Table. 2). It is

Table 2. The particulars of behavior and properties of the system PBG-DMF below and above the concentration region in the vicinity 63% of PBG.

	$V_2 \leq 63\%$	$V_2 \geq 63\%$
LC phase Fluid liquid	A broad two-phase region Turbid elastic gel	At all studied temperatures Consistency varies from paste-like to solid, transition from the turbid non-fluid state to the fluid never observed
One strong reflection on the WAXS patterns with concentration- dependent position	Two strong reflections on the WAXS patterns with concentration-independent positions; WAXS corresponds to the mixture of LC and “complex” phase	Superposition of reflections of crystalline and “complex” phase on the WAXS patterns

the domains of “complex” phase or crystallosoolvates that apparently form the gel network nodes.^[18]

Finally, one more piece of evidence for the important role of crystallosoolvates is the virtually coinciding shapes of the qualitative PD proposed by Papkov for the solutions of rodlike macromolecules [constructed by him by taking into account the combination of various types of the phase equilibria,^[1,3,76] in particular with an allowance for the possible formation of crystallosoolvates; see Fig. 5] and the generalized PD (Fig. 20).

5.2. Generalized Phase Diagram

Figure 20 shows the most complete (at present) PD of the PBG-DMF system; it was plotted on the basis of the entire body of experimental material presented above. This shape of the PD is typical of PBG with sufficiently high molecular mass ($2 \times 10^5 - 3 \times 10^5$).

According to the experimental data and in full accordance with the concept of combination of various types of phase equilibria, the generalized PD of the system under consideration exhibits two homogeneity regions, corresponding to the isotropic liquid (I) and liquid crystal (LC), and five two-phase regions: isotropic liquid plus liquid crystal (I + LC), isotropic liquid plus crystallosoolvate (I + CS), liquid crystal plus crystallosoolvate (LC + CS), crystal plus crystallosoolvate (Cr + CS), and crystal plus liquid crystal (Cr + LC).

5.3. Classification of the Different Structure Units in the PBG-DMF System

Let us consider the region of the PD with concentrations in the vicinity of V_2^{CS} and temperatures above T_2 in Fig. 20, corresponding to the triple point D. Imagine

Phase Diagram for System of PBG/DMF

29

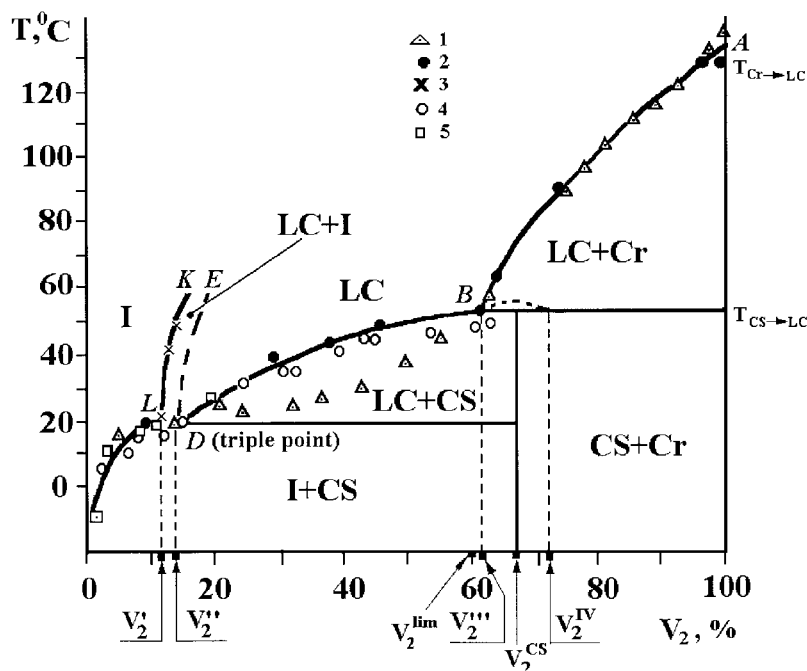


Figure 20. Schematic phase diagram based on a combination of the experimental data obtained for the high-molecular-mass PBG solutions. $M = (2-3) \times 10^5$. (1) DSC^[18,61], and other data taken from^[64,97]; (2) DSC; (3) optical data revised by us; (4) turbidity point and fluidity loss methods; (5) detection of the gel formation by probing mechanical properties (rebound of a steel ball).

the possible structural units which the system can be composed of. If we assume that the structural units of the crystallosolvate phase comprise, in accordance with the x-ray data, a combination of two PBG repeat units and three DMF molecules then the PBG mass fraction in CS is exactly $V_2^{CS} = 2/3$ (or $\sim 66.7\%$). The scheme of this structure unit is shown in Fig. 21b. In order to permit the CS phase to convert completely into an LC phase upon dilution, it is necessary to add at least one solvent molecule to the CS structural unit (Fig. 21a). The LC phase composed completely of these structural units will be termed the limiting LC phase. The polymer concentration in the limiting LC phase amounts to $V_2^{lim} = 60\%$. Structural units (Fig. 21c) obtained upon subtracting one solvent molecule from the CS structural unit will be referred to as the “semidry” units. The polymer concentration in the semidry LC phase is 75%. “Dry” systems comprising a single solvent molecule per two PBG repeat units (Fig. 21d) contain 85.7% of the polymer. Finally, the “crystal-like” structural units (Fig. 21e) contain 100% of the polymer.

As we can see in the next section a similar classification of structure units can be useful for understanding the PD features.

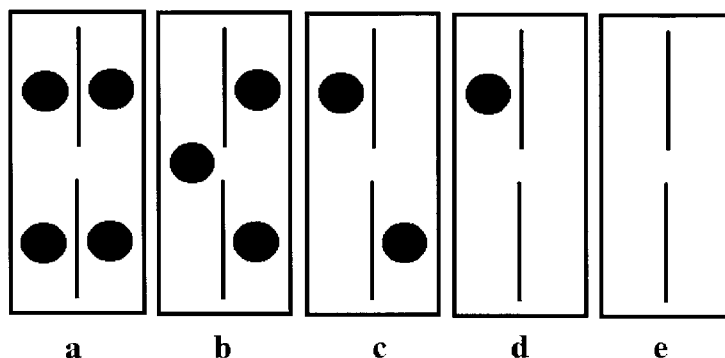


Figure 21. Schemes of conventional structure units in PBG-DMF system: rods are the repeat units of PBG, circles are molecules of DMF; (a) limiting LC phase; (b) crystallosolvate phase; (c) semidry structure units; (d) dry structure units; (e) crystalline phase.

5.4. Concentration and Temperature Transitions in the High Concentration Region

Following Papkov^[4] we denote the concentrations V_2^{III} and V_2^{IV} in Fig. 20. The concentration of the “limiting” LC phase $V_2^{\text{lim}} = 60\%$ is very close to concentration $V_2^{III} = 63\%$. Let us consider this part of the PD in more detail (Fig. 22). During heating of the system with a concentration $V_2^{\text{lim}} = 60\%$ and at its transition from the region (LC + CS) into the LC phase a melting occurs at the point B' and the melt formed in an ideal case will consist only of the structure units of the “limiting” LC phase. In the case of melting of more concentrated systems the other types of the structure units must of necessity exist with a lower solvent content. Nevertheless, at concentrations near $V_2 \sim 60\%$ the sharp changes of different properties (rheological, mechanical, optical, thermal) which have been observed for this system at $V_2 \sim 63\%$ ^[64,98] do not occur (see Table. 2). Apparently, for these changes, a sufficiently large fraction of the CS phase is required in the system. Simple calculation shows that 3 wt% of polymer added to the concentration of the “limiting” LC phase can form in the system up to 48 mol.% of the structure units of the pure CS phase. During heating of the system with $V_2 = 63\%$ at point B'', 48 mol.% of CS phase and 52 mol.% of the “limiting” LC phase will form.

Thus, the structure interpretation of V_2^{III} as the concentration at which a sufficiently large fraction of CS phase forms to sharply change the physical properties of the system is clear.

V_2^{IV} is a concentration corresponding to one more possible sharp change of the system properties at a sufficiently large fraction of the “dry” defect units of the CS phase. However no experimental evidence for this concentration has been seen up to now. It is clear only that it should be located between $V_2^{\text{CS}} = 66.7\%$ and the concentration corresponding to 100% of nonequilibrium “semidry” defect units of CS phase ($V_2 = 75\%$). At concentrations $V_2 > 75\%$ some fraction of crystal-like structure units always occurs.

Possibly one experimental evidence of V_2^{IV} is that in the concentration interval from 60% to 72% (i.e., to near V_2^{IV}) the DSC diagrams are very diffuse and their usage for

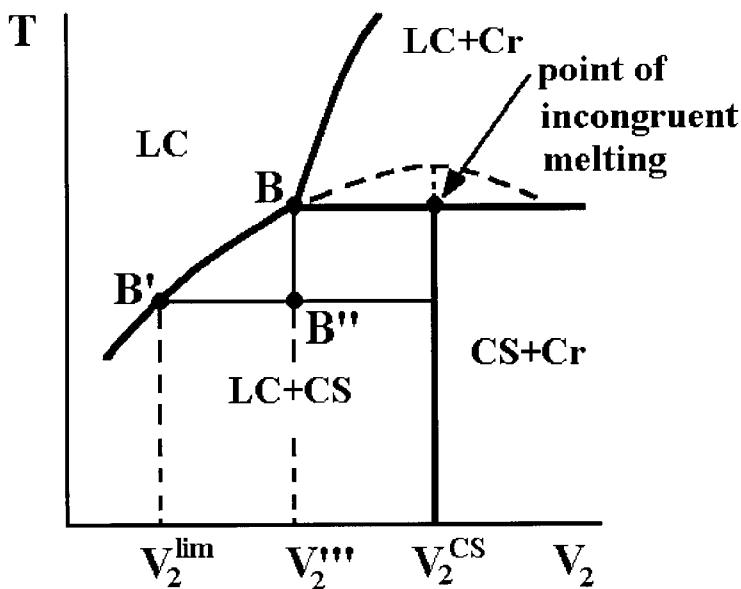


Figure 22. A part of the phase diagram, shown in Fig. 24. V_2^{lim} is the concentration of PBG corresponding to the “limiting” LC phase; $V_2^{\text{'''}}$ is the concentration, corresponding to the boundary of congruent and incongruent melting of gels; V_2^{CS} is the concentration corresponding to 100% of crystallosolvate phase.

the determination of transition temperatures presents a problem. Let us remark also that V_2^{IV} is a hypothetical eutectic concentration of the mixture of crystallosolvates and crystallites if the former should melt congruently.

Now let us discuss in more detail the special features of the temperature transitions in the region of high values of V_2 . In the region $V_2 \leq V_2^{\text{'''}}$ heating of the systems located in the area (LC + CS) of the PD must lead to a congruent melting of the crystallosolvates (representing the junctions of the gel network), i.e., without their degradation into the components, PBG and solvent, and to a transition of the system from the biphasic state (a mixture of CS phase and relatively diluted LC phase) to a single LC phase with a concentration corresponding to the given value of V_2 .

In the concentration interval $V_2^{\text{lim}} < V_2 < V_2^{\text{CS}}$ the heating must lead to an incongruent melting of the gels, i.e., to a melting which must be accompanied by a degradation of the CS phase into solvent and polymer. In so doing, part of the components form a new LC phase with a polymer concentration $V_2^{\text{'''}}$ in it, and the other one forms a crystal phase melting in the process of the following heating to higher temperatures. In the concentration interval $V_2^{\text{CS}} < V_2 < V_2^{\text{Cr}}$ the heating must lead to an incongruent melting of the CS phase. Instead the CS phase must yield the LC phase and an additional fraction of the crystal phase. Thus, the concentration $V_2^{\text{'''}}$ divides the areas of congruent and incongruent melting of the CS phase.

Some quantitative evaluations of the phase composition forming during the melting and following degradation of the CS phase are schematically represented in Fig. 23.

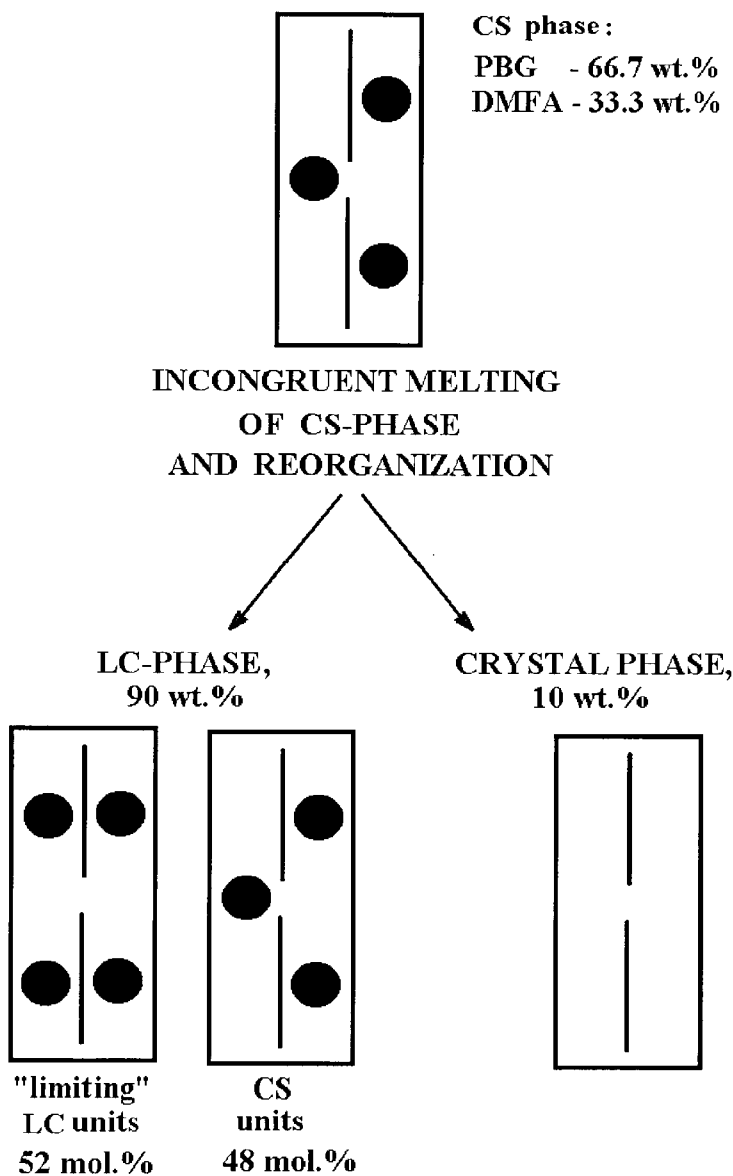


Figure 23. Scheme of a component redistribution during incongruent melting and the following reorganization of the crystallosolvate phase.

During melting of the 100% CS phase, one part of the polymer with all corresponding solvent goes into formation of the LC phase (consisting of 52 mol.% of the structure units of the "limiting" LC phase and 48 mol.% of CS structure units), and the remaining part of the "dry" polymer can form the crystalline phase of PBG.

Phase Diagram for System of PBG/DMF

33

From this consideration the existence of two peaks in DSC diagrams in the concentration interval from 63% to 67% become understandable (see Fig. 14): the first peak is related to a CS melting and the second one (or the high-temperature shoulder) apparently is related to crystal phase melting. If the temperature scanning rate is too quick the processes of structure transformation (melting of the CS phase, forming of the LC phase, and forming and melting of the crystal phase), taking place in a relatively short temperature interval, can lead to the smearing of the peaks in DSC diagrams. Just this factor was shown by the authors in Refs.^[18,61] and apparently this is a reason that they did not show their DSC results in the $58\% < V_2 < 72\%$ region (see Fig. 13).

In the concentration region $V_2 < V_2^{CS}$ the fraction of the crystal phase, forming immediately after the CS melting, is relatively small (Table. 3); however, for a variety of reasons (for example, the large viscosity of the system, hindering the crystallization) the concentration of a new forming crystal phase can be even smaller. Hence, at $V_2 = 64\%$ it can reach a maximum value $\sim 3.0\%$ (see Table. 3) but apparently in the real experiment it does not form at all and DSC diagrams can record only one peak which reflects the melting of the CS phase and the transition of the system into the LC phase. It can be proposed that instead of the 3% of crystals a corresponding fraction of more solvent-rich structure units is produced. At higher concentration of PBG (but less than V_2^{CS}) the maximum value of new forming crystals is also not very large, not more than 8–10% at the common polymer concentration of 64–66% (see Table. 3). Thus, the exothermic effect of crystallization

Table 3. Calculated relationships of the phases during melting of the crystallosolvate phase in concentrated ($V_2 \geq 60\%$) system PBG-DMF. Notation: LC = fraction of LC phase; CS = fraction of crystallosolvate phase; Cr = fraction of crystalline phase; Cr_0 = maximal common fraction of crystalline phase after the melting of crystallosolvate phase; Cr' = maximal fraction of the new crystalline phase, formed after melting of crystallosolvate phase. All fractions are given in the weight percents.

N	Before the melting of CS-phase				After the melting of CS-phase			
	V_2	LC	CS	Cr	LC	Cr_0	Cr'	$(Cr'/CS) \times 100$
1	60.0	12.9	87.1	0	100	0	0	0
2	62.8	7.5	92.5	0	100	0	0	0
3	63.0	7.2	92.8	0	100	0	0	0
4	64.0	5.2	94.8	0	97	3	3	3
5	66.0	1.4	98.6	0	92	8	8	8
6	66.7	0	100	0	90	10	10	10
7	70.0	0	90	10	81.1	18.9	8.9	10
8	72.0	0	84	16	75.7	24.3	8.3	10
9	76.0	0	72	28	64.9	35.2	7.2	10
10	82.0	0	54	46	48.7	51.3	5.3	10
11	88.0	0	36	64	32.4	67.6	3.6	10
12	94.0	0	18	82	17.2	83.8	1.8	10
13	96.0	0	12	88	10.8	89.2	1.2	10
14	98.6	0	6	94	5.4	94.6	0.6	10
15	100	0	0	100	0	100	0	—

cannot compensate the endothermic effect of CS melting. Then two endothermic peaks are observed in DSC diagrams corresponding to melting of the CS phase and, at a higher temperature, to melting of the crystal phase; both phases transform into the LC phase.

During melting of pure CS phase (at polymer concentration V_2^{CS}) the maximum amount of crystal phase that forms is 10%. With further increase in initial polymer concentration the fraction of crystal phase (forming at the transition through the temperature T_{CS}^d and melting of the CS phase) decreases again. However, with increase in the initial polymer concentration the initial fraction of the CS phase also decreases and, relative to it, the fraction of forming crystal phase remains constant ($\sim 10\%$, see Table. 3). Obviously, this amount of the crystal phase is sufficient such that the exothermic effect of crystallization would be comparable with the endothermic effect of melting of the CS phase. This can be one of the reasons that some strong thermal effects are not observed at the transition from the two-phase region (CS + Cr) into the two-phase region (LC + Cr). The only peak observed on the DSC thermograms corresponds to the melting of crystallites and the transition of the system into LC monophase.

Similar considerations can be applied to the transitions between the regions (I + CS) and (LC + CS): a partial melting of CS must occur simultaneously with the forming of the LC phase. A question arises on the nature of the LC monophase forming from the two phase region (LC + Cr) at polymer concentrations exceeding its concentration in the "limiting" LC phase. In the more general case at $V_2 \geq V_2'''$ melting of the crystal phase occurs with its transition into an LC phase containing no solvent (though immediately diluted by the solvent); in other words, a thermotropic transition occurs. Thus a transition (LC + Cr) \rightarrow LC can be considered as thermotropic according to the earlier Papkov concept.^[3,76] Liquidus curve on the considered PD and the existence of the transition temperature $T_{C \rightarrow LC}$ for the melting of pure crystals into thermotropic LC, in our opinion, are the experimental confirmation of this hypothesis. Thus, the assignment of the rodlike polymer solutions to lyotropic systems is wrong from the scientific point of view and can be used only for an indication of the technological method of their preparation.

Note that the thermotropic LC state in rodlike polymer systems sometimes cannot be realized owing to two reasons. The first one is a thermal degradation of chemical structure of the polymer chains before the melting. The other reason is a monotropicity that was observed in low molecular LC phases. In the latter case, evidence of a possible LC state and determination of its possible kind can be obtained through the mixture with in other LCs with known structure, analogously as it is usually carried out for low molecular LC.^[117]

The temperatures $T_{C \rightarrow LC}$ determined by three groups of authors,^[18,61,62,64,118] on the one hand, are very similar (137°C, 130°C, and 130°C) and on the other hand, the scattering of the results is not accidental and reflects the effect of molecular mass.

5.5. Temperature of Isotropic Liquid-Gel Transitions at Concentrations Below the First Critical Concentration

At first sight a low concentration region appears to be investigated best of all, because it is this region that has been studied the most in the literature (see, for instance, Refs.^[54-64,84,106], etc.). However, strange as it may seem, it is this region, in our

Phase Diagram for System of PBG/DMF

35

opinion, that has the most uncertainty. For instance three types of shape of phase equilibrium curves have been experimentally observed between an isotropic phase and a two-phase region (I + CS): a curve with a maximum (see Fig. 8b, c), a curve with a “horizontal step” and equality of T_1 and T_2 temperatures (see Fig. 20), and a curve with a “vertical ledge” and different T_1 and T_2 temperatures (see Fig. 9).

Apparently there are two kinds of possible reasons which can influence the mentioned variety of shapes of experimental curves. One kind is related to the kinetic character of the thermal prehistory of the samples. The other kind is related to the molecular mass effect on the transition temperatures of the CS phase and correspondingly on the position of CS-LC and CS-I liquidus curves.

Consider these assumptions in more detail. Let us begin from the curves with a maximum in the considered region of concentrations (Fig. 24a). For the explanation of the curves of this type it is necessary to assign one more equilibrium with upper critical point between two isotropic solutions. Naturally, this equilibrium is only potentially possible, though it occurs very often in practice.^[5] However, its influence can be distinctly exhibited^[5] if a binodal lies not far below the liquidus curve CS-I along the temperature scale.

The rate of the formation of crystallization nuclei (or of the nuclei of crystallo-solvates formation) during solution cooling can be insignificantly small, especially in the low polymer concentration region.

However, if crystallization occurs in the area of potential stratification of isotropic liquid (below the mentioned binodal), then the stratification of isotropic liquid become the reality and immediately accelerates a crystallization process, because the rate of crystal nucleation is higher in the more concentrated solution.

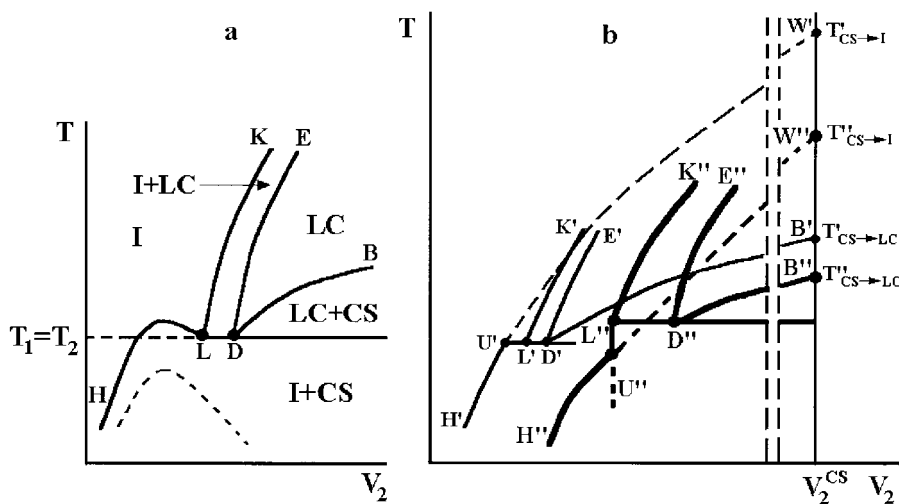


Figure 24. Examples of various shapes of phase equilibrium curves in the low concentration region between isotropic liquid and two-phase region (I + CS): a curve with a maximum (a), by the dashed line an equilibrium curve is shown, between two parts of disintegrated solution with upper critical points; (b) the curves with a horizontal step $U'L'$ (upper PD) and vertical ledge $U''L''$ (lower PD, bold lines).

Apparently this situation has been observed in Ref.^[57], where a gel formation in this PD region was studied during cooling by recording visually beginning and end of the process. In Fig. 8c the experimental curves have a distinct maximum, the shape of which obviously repeats the shape of an equilibrium curve between two isotropic liquids. Inasmuch as the curve of crystallization temperatures repeats the shape of that equilibrium curve, the curve of melting temperatures (Fig. 8b) could contain this information as a thermal prehistory.

Consider now some examples of the assumed effects of PBG molecular mass (Fig. 24b). In the case of high molecular mass, the liquidus $W'H'$ of the equilibrium CS-I apparently is higher than in the case of lower molecular mass (liquidus $W''H''$) and crosses the narrow two-phase corridor so that the horizontal step $U'L'$ forms on the equilibrium curve I-(I + CS). In the case of low molecular mass this step does not form, but on the equilibrium curve a peculiar kind of “vertical ledge” $L''U''$ can be observed.

Note that, in accord with our assumption, the CS-I liquidus always is steeper than the CS-LC one, and the corresponding hypothetical transition temperature $T_{CS \rightarrow I}$ lies above $T_{CS \rightarrow LC}$. In our mind, this assumption is confirmed by the calculation of Balby^[73] from which follows the same conclusion.

As for the transition temperature $T_{CS \rightarrow I}$ we suppose that this temperature must coincide with the temperature $T_{LC \rightarrow I}$. One of the arguments in support of this point of view is the approximate equality of transition temperatures of crystal phase into isotropic liquid and isotropic liquid into monotropic LC in mesogenic low molecular mass compounds. However, in any case, both liquiduses and transition temperatures must lie above for a high molecular mass polymer than for a low molecular one.

5.6. Metastable Gels Region

Let us consider some features of the experimental obtaining of true equilibrium curves in the PD with different shape in the low concentration region.

5.6.1. Phase Diagrams with the Horizontal Step

Consider the PD in Fig. 25a. Let us select a solution with some y -th concentration, V_2^y , and begin to cool it from the point Y, that is from the temperature T_1 in the isotropic phase, to the temperature T_{I+CS} .

In this case it is necessary to consider a set of possible experimental results determined only by the kinetics of the processes occurring in the system.

Let us decrease the temperature of isotropic liquid (sufficiently slow for a quasi-equilibrium state to establish at each temperature step). After reaching the narrow biphasic region the system divides into two phases with polymer concentrations V_2^l and V_2^h ; then these phases will be cooled and their configuration points in the PD will move along the corresponding branch of the narrow biphasic region toward the points L and D, located at the temperatures T_1 and T_2 respectively, though in this particular case $T_1 = T_2$. The LC phase at point D, owing to its higher order, has a greater tendency to crystallization (formation of crystallosolvates); hence with further temperature decrease it forms

Phase Diagram for System of PBG/DMF

37

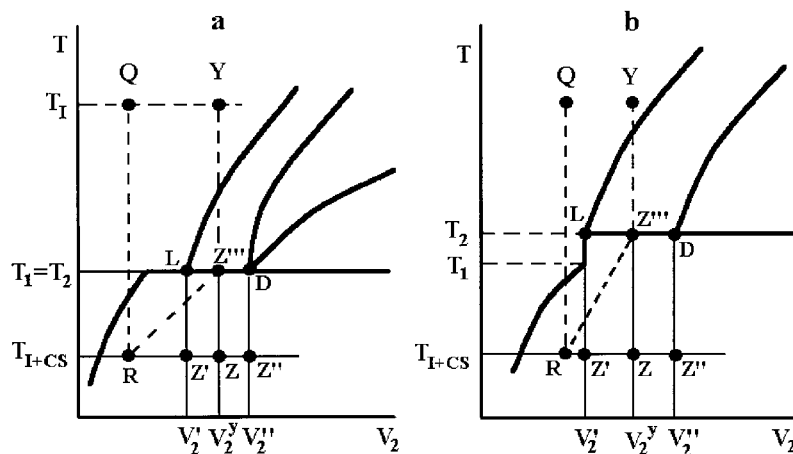


Figure 25. Preparation of equilibrium gel systems and hypothetical schemes of the ways of corresponding configuration points along the phase diagrams: (a) with a horizontal step and (b) vertical ledge. For additional explanations see the text.

(quickly or with a small overcooling) gel. At the same time the isotropic phase, located at point L, as a phase without any long-range order and more diluted, has significantly more tendency to overcooling than the LC phase.

Nevertheless, in the case of quasi-equilibrium cooling one would expect almost simultaneous solidification of both phases. This is likely, because the interface can serve as a center of crystallization in the isotropic phase. However, even in the state of a common gel, a two-phase state and a dividing of the system into two parts (points Z' and Z'') will be fixed as in the previously considered region of the PD.

Each of the forming gels is also a two-phase system with its own relationship of the components determined by concentrations V_2' and V_2'' . Because in the case of high molecular mass of the polymer these concentrations are very close to each other, therefore gels, formed from isotropic and anisotropic phases, have almost the same composition and properties. Nevertheless the “memory” of the previous two-phase state makes the common gel, strictly speaking, a nonequilibrium gel from the thermodynamic point of view, though it is stable in time owing to loss of its fluidity. Even a following annealing can be only a little effective. Thus a quasi-equilibrium cooling of a two-phase system of this type can lead to a nonequilibrium gel.

Consider a variant of quick cooling, during which the system does not have time for dividing into two macrophases. In Fig. 25a the quick cooling is reflected in the transition of the system from point Y into point Z. From the position of point Z it is clear what relationship will arise during microphase separation of gel on isotropic and CS phase. By means of subsequent annealing this gel can be transferred into the state as close as one likes to equilibrium (point Z'''); this will give the same melting temperature for all solutions (gels) with concentrations between V_2' and V_2'' . However, another variant is possible for obtaining a thermodynamically equilibrium state in this concentration interval. It is possible to carry out the cooling of the isotropic liquid at sufficiently low

concentration so that a single gel forms through the whole sample (a way from point Q to point R in Fig. 25a). Then, removing the solvent vapors and heating the system (sequentially or simultaneously) one can obtain equilibrium gels, including as close as is wished to the phase equilibrium curve between the gel and narrow biphasic region (for instance, by RZZ''' or RZ''').

5.6.2. Phase Diagram with a Vertical Ledge

In the case of the PD with a “vertical ledge”, a stratification of gels, forming during quasi-equilibrium cooling, will be much more pronounced than in the previous case. This is due to the fact that PDs of this type can be observed most probably for solutions of relatively low molecular mass PBG (see Fig. 13). For such solutions the narrow biphasic region is much wider and temperatures T_1 and T_2 differ significantly.

Thus, during quasi-equilibrium cooling of the sample from a narrow biphasic region and its transition across the temperature T_2 (Fig. 25b), gel forms in the anisotropic part. At the same time, the isotropic phase remains fluid and equilibrium up to the temperature T_1 when the left branch of the narrow biphasic region crosses the liquidus line CS-isotropic liquid.

Below T_1 the sample will consist of two gels as in the previous case. Thus, the state of the sample is not reflected by any configuration point in the concentration interval between V_2' and V_2'' . During heating of such a sample, a melting of its different parts will occur in the reverse sequence, first a less concentrated gel at T_1 , and then a more concentrated gel at T_2 . For preparation of a thermodynamically equilibrium single gel through the whole sample the same techniques can be applied as described in the previous case. Then the equilibrium gel will give the same melting temperature during heating of all systems within the concentration interval between V_2' and V_2'' .

Thus, to obtain equilibrium gels an unusual way is required. This feature is determined by the necessity of transition of the system from one two-phase region to the other one with a simultaneous loss of the fluidity.

Let us point out that a decrease in molecular mass (in addition to the enumerated earlier effects on a narrow biphasic region) leads to an increase in the difference $T_2 - T_1$.

5.7. The Results of DSC Studies

Some special features of thermograph studies of binary systems have been considered in the literature.^[119] Ignorance of these features can lead to incorrect setting up of experiments and to misinterpretation of experimental results. In particular, during the transition through a two-phase region in a PD with a crossing of two equilibrium curves, DSC diagrams very often give only one peak. On the other hand, the presence of a singularity similar to a peak in these diagrams does not mean unambiguously a crossing of a phase equilibrium curve.

Consider some theoretical thermograph results, directly relating to the topic of this paper. Figure 26 shows a typical scheme of the PD of binary systems with a simple eutectic point (Fig. 26a), and schemes of corresponding changes of the heat capacity C_p (Fig. 26b),

Phase Diagram for System of PBG/DMF

39

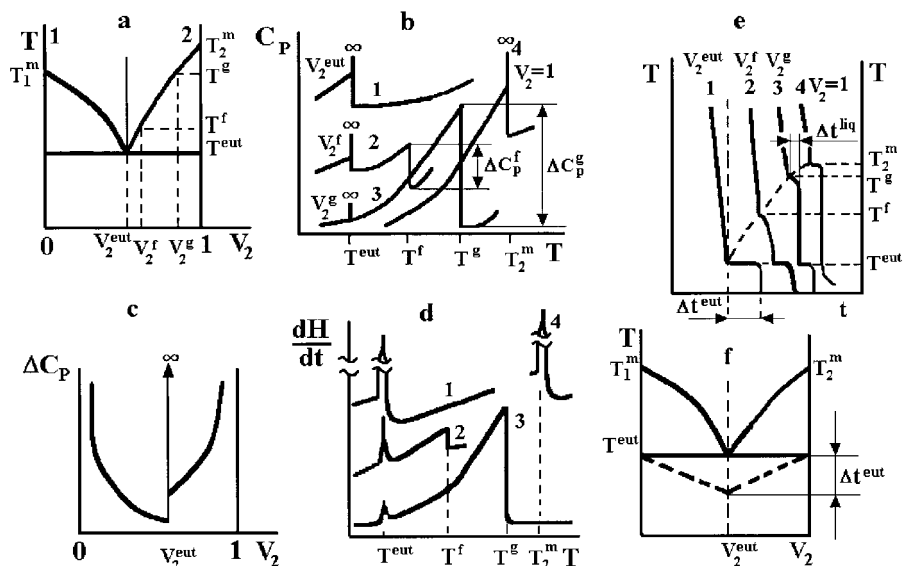


Figure 26. Schemes illustrating the special features of thermal measurements in binary systems: (a) the phase diagram of a binary system with a simple eutectic for components 1 and 2; (b) the heat capacity C_p versus temperature for different volume fractions of component 2 (see the text); (c) the jump of the heat capacity ΔC_p (at the transition through the liquids) versus volume fraction; (d) the heat generation versus: temperature in DSC thermograms; (e) temperature of the system versus time (T - t diagrams); (f) connection of the phase diagram with T - t diagrams; schematic dependence of melting time versus V_2 is shown by dashed line.

concentration dependence of the jump of the heat capacity ΔC_p at the transition from heterophase region to monophasic (Fig. 26c), DSC curves (Fig. 26d), T - t diagrams, where t is a time (Fig. 26e), and connection of the PD with the T - t diagram (Fig. 26f).^[119]

Consider these schemes for heating of systems which are initially below the eutectic temperature T^{eut} and have an eutectic concentration V_2^{eut} of the component 2 (Fig. 26a). During passage through the temperature T^{eut} a jump of heat capacity ($C_p \rightarrow \infty$) occurs in the form of a δ -function (Fig. 26b, curve 1); with further temperature increase the value C_p in a liquid monophasic also smoothly increases. Only one sufficiently sharp peak, corresponding to a δ -like jump of C_p , will be observed on thermograms (Fig. 26d, curve 1). On T - t diagrams a horizontal step will arise (Fig. 26e, curve 1), the length of which corresponds to the time of a sample melting Δt^{eut} .

Consider a case when the composition of a system differs from eutectic (for example, at concentrations V_2^f and V_2^g of component 2). The character of the temperature dependence of C_p changes significantly: in addition to a δ -like jump at T^{eut} there is a λ -like singularity rises with a sharp drop in the value ΔC_p during the transition through a liquidus curve (at temperatures T^f and T^g corresponding to the selected composition of the mixture) (see Fig. 26b, curves 2 and 3). Similar changes are observed on DSC curves (Fig. 26d, curves 2 and 3). On the T - t diagrams bending and a smeared step arise with a length Δt^{liq} at the same temperatures and in addition to a horizontal step at the T^{eut} .

Besides, for deviation of a composition from an eutectic one the intensity of a δ -like jump of a heat capacity decreases directly proportional to the part of the sample which has a eutectic composition, and a λ -like jump, vice-versa, increases in intensity (Fig. 26b, c, and d), and its shape approaches to δ -like one. Accordingly the DSC peak intensity decreases (Fig. 26d, curves 2 and 3). On T-t diagrams the length of the horizontal step Δt^{cut} , corresponding to the melting time of the sample fraction with an eutectic composition, decreases (Fig. 26e, f).

Finally, at $V_2 = 1$ there is only one δ -like jump of heat capacity (Fig. 26b, curve 4), one peak in DSC thermograms (Fig. 26d, curve 4), and also the only horizontal step on the T-t diagrams (Fig. 26f, curve 4), corresponding to a melting of a pure component 2.

Thus, the λ -shaped jump of ΔC_p is small in the vicinity of the eutectic point (Fig. 26b, curve 2, and Fig. 26c) and a peak-shaped singularity on DSC thermograms (Fig. 26d, curve 2) is correspondingly small. Therefore a recording of liquidus crossing near the eutectic point by DSC is hindered, especially at high-temperature scanning rates. On the other hand, far from the eutectic composition (e.g., at V_2^g) and at high-temperature scanning rates, a recording of the transition through the T^{cut} (Fig. 26d, curve 3) can be hindered because the system has a small part with eutectic composition. Similar problems arise during determination of T-t diagrams (Fig. 26e).

Problems of recording of transitions between the regions of phase diagrams by DSC can be related not only with the δ -like feature of heat capacity jump at T^{cut} , but also with a redistribution of different phases during the heating or cooling of the system, in the two-phase region. On approaching the liquidus, in accordance with the lever rule, too small an amount of the melting phase in the system remains. Accordingly the thermal effects must be small, which is reflected on the T-t diagrams.

However here, at high-temperature scanning rate, it is easier to record this transition by DSC because, during the approach to phase equilibrium curve, a melting phase is maintained to a higher degree. Therefore, we suppose that the dependence of properties of concrete systems on the temperature scanning rates in DSC experiments must be various in different ranges of the phase diagrams.

In this relation let us return to a discussion of the experimental data obtained by two groups of authors for PBG-DMF systems (see Fig. 13).

Apparently, the rate of sample heating used in Ref.^[64] (5°C/min) was too high, and only points where the system passed through a liquidus were detected. As noted above, reliability of the results reported in Ref.^[64] was proved by different methods detecting the gel formation on the liquidus curve between crystallo-solvates and isotropic liquid.

The heating rate used in Refs.^[18,61] was probably lower and the results obtained in the concentration interval 20–40% most likely refer to transition from (I + CS) to (LC + CS). However, the heating rate, although sufficiently low for the above concentration range, could be too high for the system to rearrange when the concentration increased further to approach the V_2^{CS} level. For this reason, the experimental points in the concentration range of 40–50% fall between the two curves of phase equilibria. In the vicinity of V_2^{CS} , a concentration corresponding to the crystallo-solvate phase, the complex character of structural rearrangements probably accounts for the difficulty in interpretation of the DSC curves. The high rate of temperature scanning may result in the structure transformation, involving the melting of crystallo-solvates, the LC phase formation, and the formation and melting of the PBG crystallites within a relatively narrow temperature

Phase Diagram for System of PBG/DMF

41

interval, which leads to smearing of the DSC peaks. This circumstance was also emphasized^[18,61] and may explain the fact that no results were reported on the determination of phase transition temperatures in the concentration interval $58\% < V_2 < 72\%$.

At still higher concentrations, the heating rate (provided it was constant) remained too fast, which hindered the detection of transitions in the solid and gel states. In our opinion, the experimental points reported for this region reflect only the transitions to a liquid-phase state upon crossing the liquidus curve. The shape of the liquidus curve plotted with the data,^[18] and a close correspondence between the melting temperature of the crystalline phase reported by the two groups of researchers, confirm the above conclusions and justify the approach used to construct the phase diagram in the range of high concentrations.

It should be noted also that, according to Ref.^[119], the heat capacity C_p for a binary heterogeneous isolated system within the two-phase region is given by:

$$C_p = \sum_{\alpha=1}^2 m_{\alpha} C_{p\alpha} + T \sum_{\alpha=1}^2 m_{\alpha} g_{xx,\alpha} |dV_2^{\alpha}/dT|_p^2 \quad (2)$$

where $\alpha = 1, 2$ are symbols of the system components, m_{α} are their molar fractions, $C_{p\alpha}$ are their isobaric molar specific heat capacities, T is a temperature, $g_{xx,\alpha}$ is the second derivative of the Gibbs energy on the change of the fraction of the α -phase, and $|dV_2^{\alpha}/dT|_p$ is the change of the fraction of α -phase with variation of the temperature.

Hence we have that the heat capacity of the system equals the sum of heat capacities of coexisting phases only in the case that a relationship between the fraction of phases does not change with temperature variations, that is, the boundaries determining this relationship in the two-phase region of the PD are vertical.

This case corresponds to heating a monophase gel from temperature T_1 to temperature T_2 on the PD with a vertical ledge, which occurs for relatively small PBG molecular masses or other polymers with a sufficiently small aspect ratio of rodlike molecules. Therefore, during passing through the system temperature T_1 , the heat capacity of this system changes by a jump that can be manifested on DSC thermograms; up to now, however, nobody has observed it.

5.8. Phase Diagrams for Some Other Systems

In this section we shall give a series of examples of PDs of rigid-chain polymer-solvent from the literature, which, in our opinion, can be corrected on the basis of our results in this paper and using the general principles of constructing PDs for binary systems.

In Ref.^[118] molecular aggregation and gel formation was investigated in the system PBG–benzyl alcohol. Figure 27 shows some parts of the PD of this system in the regions of high ($>60\%$) and low ($<10\%$) concentrations. The experimental points for high concentrations are taken directly from Ref.^[118], but points for low concentrations are the result of our rearrangement of the series of plots of temperature dependencies, shown in Ref.^[118], of shear modulus for gels in PBG (with $M = 1.5 \times 10^5$) solutions of various concentration. In this case only the points in the curves lying just before the melting were

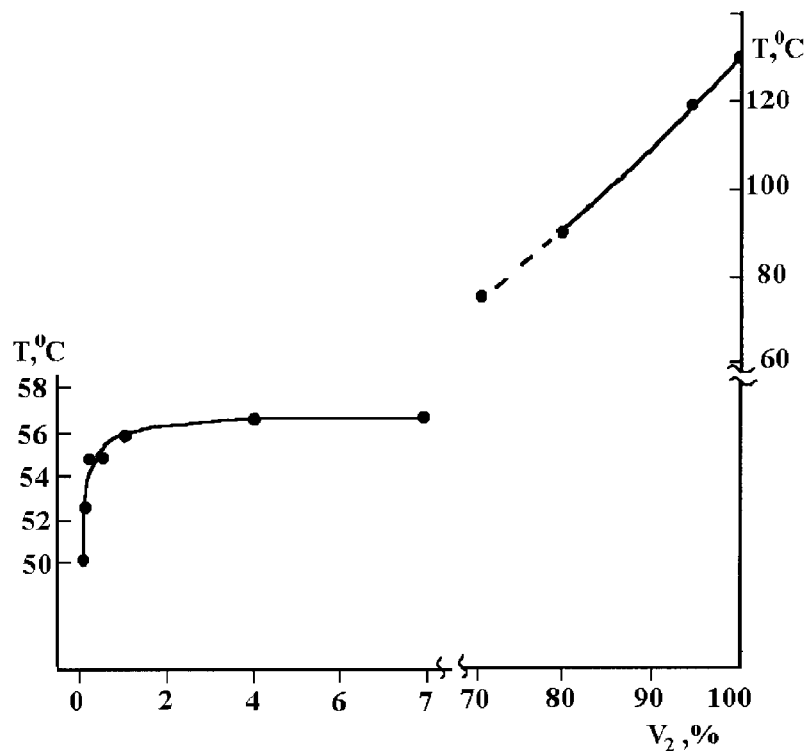


Figure 27. Phase diagram for the system PBG-benzyl-alcohol and constructed on the base of data obtained in Ref.^[118]. See the text.

used. Of course, the obtained curve is conventional but it is close to the real equilibrium curve. It is seen from Fig. 27 that the considered fragments have only small discrepancies from corresponding parts of the generalized PD. Especially note that the temperature transition from homopolymer into the thermotropic LC melt in Fig. 27 is at 130°C in good accordance with the results for the PBG-DMF system.^[64]

Phase diagrams of the poly(p-phenylene terephthalamide)- H_2SO_4 system were studied in Ref.^[119]. In particular, the equilibrium boundaries between the CS-containing regions were investigated. Figure 28 shows two plots of melting temperature of CS phase vs. concentration for polymers with molecular mass 4.48×10^4 and 3×10^4 . In our opinion these curves differ significantly.

Consider curve 1. Among the experimental points there is a sharp drop from the curve for the point near $V_2 = 15\%$ (point A). However we think that point A is not a result of data scattering and should not be averaged with the others during plotting. In the same figure we plot, by dashed lines, the equilibrium curves on the basis of our understanding of the situation. We also added some neighboring parts of the common PD although we understand that the PD may be only approximately plotted because of a deficiency of experimental points. As follows from the dashed lines in this figure it is possible that there are three different equilibria: (1) between monophasic-region I and two-phase region

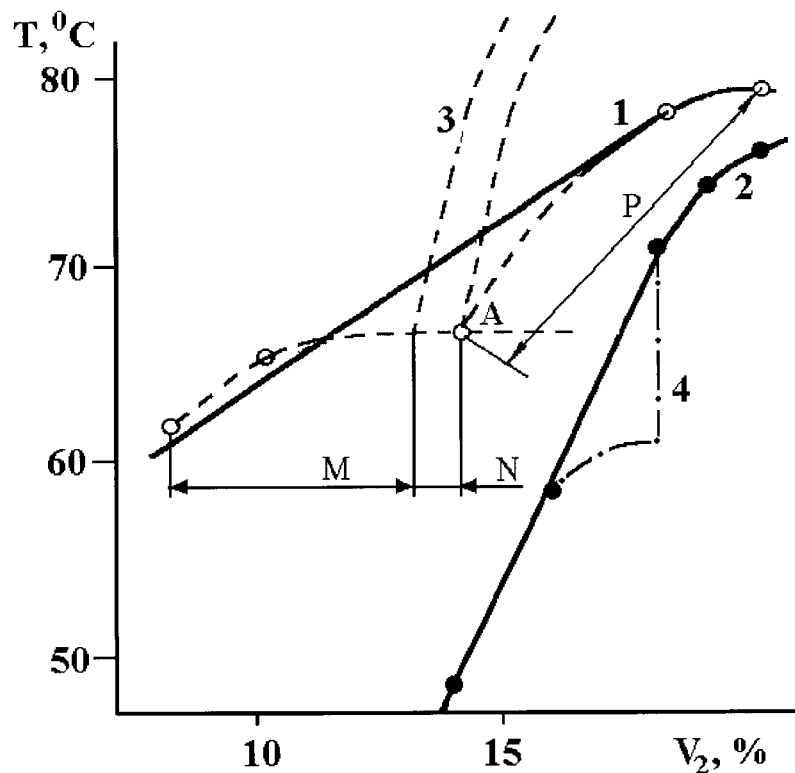


Figure 28. Plot of melting temperature versus concentration for crystallites in the system poly(phenylene terephthalamide)— H_2SO_4 . All points and bold solid lines are the data from Ref.^[119] for the polymers with molecular mass 4.48×10^4 (1) and 3×10^4 (2). Dashed (3) and dash-dotted (4) lines is a schematic representation of the part of the PD on the base of the same experimental points in accordance with an idea on a “horizontal step” (3) and “vertical ledge” (4) in the PD. For additional explanations, see in the text.

(CS-I) (section M); (2) between two-phase regions (I + LC) and (I + CS) (section N); and (3) between two-phase region (LC + CS) and monophasic-region LC (section P). Note that point A most likely does not mean any critical concentration and is only close to one of them. The PD presented here has a “horizontal step” which corresponds to higher molecular mass, as could be expected.

Now consider curve 2. In this case we also have a great deficit of experimental points but it appears that this curve is more similar to a PD with a “vertical ledge” characterizing polymers with low molecular mass. The presented experimental points, as a minimum, do not contradict the proposed classification of PD details.

In the work by Park et al.^[116] the structure and morphology of an aromatic polyimide/m-cresol system was studied. In Fig. 29a is shown the PD, plotted by the authors, in correspondence with their experimental data. On this PD the authors presented five ranges: area of isotropic solution (I on the PD); area of existence CS of one type

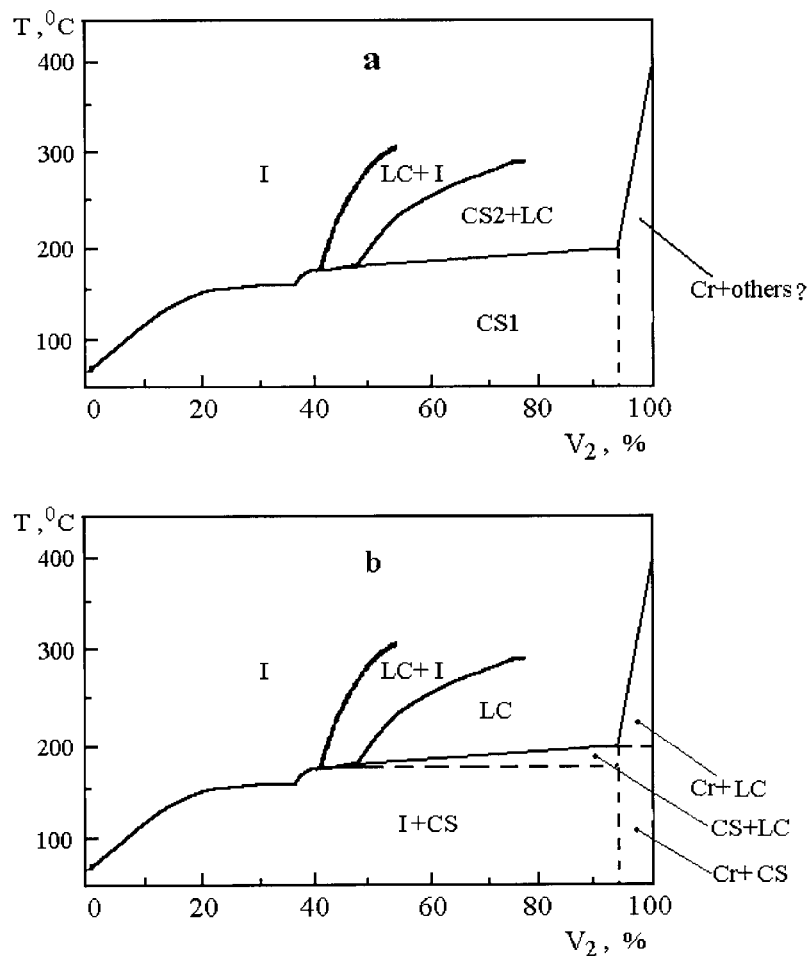


Figure 29. Phase diagram for the system aromatic polyamide—m-cresol. a—interpretation of the experimental data by the authors of Ref.^[116]; b—correction of this interpretation in accordance with concepts given in this paper. See also the text.

(CS1); area of coexisting of LC phase with CS of the other type (CS2 + LC); area of coexisting of LC with isotropic solution (LC + I) and, last, area of existence of a crystalline phase (Cr), where, in the opinion of the authors, the capability of existence also of other phases is not eliminated. Their presence could not be revealed by the x-ray scattering method and polarized optical microscopy used.

We shall carry out an analysis of the presented results. First of all, the PD should be corrected in correspondence to the common views about the PD's of binary systems. According to these representations two monophasic areas cannot be placed alongside each other—between them there should always be a biphasic area. Therefore monophasic area CS1 should be exchanged with a biphasic area of (I + CS1). Besides, the transition from

one biphasic area into the other one cannot be accompanied by a simultaneous change at once of both phases. Therefore between areas (I + CS1) and (CS2 + LC) there should be one more biphasic region (LC + CS1).

Here it is necessary to note that the conclusion about the existence of two types of CS the authors made was on the basis of an observation of two types of spherulites—negative and positive (on the sign of a birefringence along radius of spherulites), in the low- and high-temperature regions of the PD. However, there was no direct x-ray evidence of the existence of two types of CS in the published paper. Besides there are, in our view, two arguments against the existence of a CS2. First, the availability of fluid positive spherulites, related to the LC phase, is not evidence of the existence of a CS phase in general. Secondly, and this is the main argument, the shape of the PD in this case would be different. It is known (see, e.g., Ref.^[11]), that an intermediate compound in the area of its existence divides the PD in T-C coordinates into two parts, each with its own eutectic point. Existence of two intermediate compounds (e.g., of the CS type) would divide it already into three parts that should be manifested in the experimental PD.

If one suggests that there is only one CS phase, the indicated difficulties in interpretation can be avoided (correction is shown in Fig. 29b): at low temperatures there is a biphasic area coexisting of isotropic solution with CS (I + CS); above it there is a biphasic area of coexisting of LC and CS phases (CS + LC), and the area of the LC phase exists at even higher temperature. Besides, in accordance with the general representations about PDs of binary systems, in this figure the areas (Cr + CS), (CS + LC), and (Cr + LC) are imaged. Thus, it becomes clear, what experimentally undetected phases it is necessary to search for in the various areas of the PD.

Among other results of the work^[116] we note the clearly visible strong bend of the narrow biphasic region toward high concentrations, that, as appears now to us, is a natural limitation of existence of the LC phase from the side of high temperatures. Further, the authors of Ref.^[116] have showed that in the low-temperature area of existence of the spherulites, gel is formed. And, finally, on the PD shown in Fig. 29 there is a clear liquidus apparently separating the area of the LC phase from the biphasic area of (LC + Cr); this is additional confirmation of the thermotropic nature and thermotropic behavior of one more rigid-chain polymer and its solution.

5.9. Main Advances and the Perspectives for Further Investigations

Figure 30 shows a PD constructed by us on the basis of the experimental literature data for the PBG-DMF system. This PD corresponds to PBG molecular mass of $(2-3) \times 10^5$ but, other than for a few exclusions, reflects also the main features of the PD for lower molecular mass PBG.

Let us discuss this PD in two aspects: what on this PD is reliably established and what is required for further refinement or can be changed by further investigations of similar systems. We note that, in our mind, the possible changes can be related mainly by taking into account the molecular mass effect and kinetics of structure changes during measurements while heating or cooling the system.

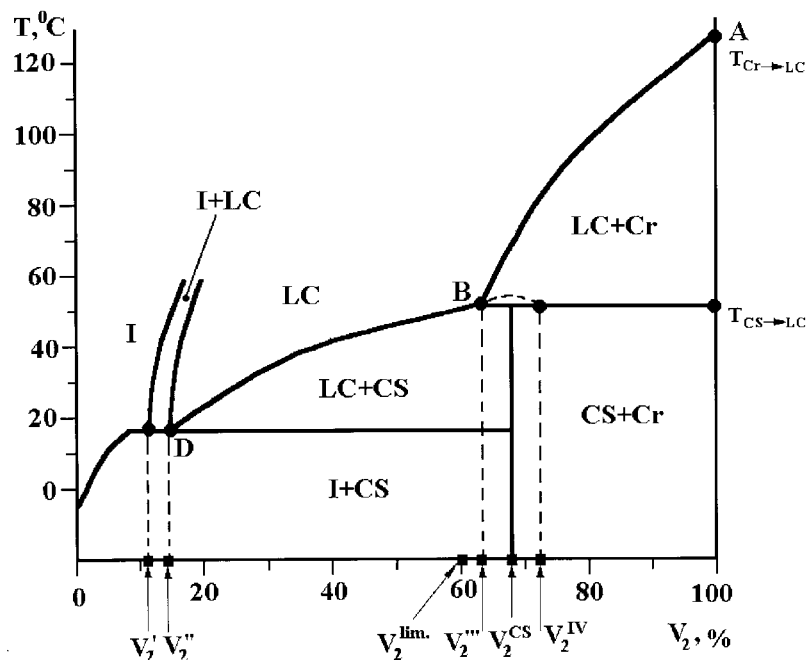


Figure 30. The final schemes of the phase diagram of PBG-DMF systems. Generalized PD, constructed on the basis of modern experimental data.

1. Three independent groups of authors^[18,61,62,64,118] have established the temperature of melting of the crystalline phase (130–137°C). Some scattering of the data may be due to the difference in molecular mass of the investigated PBG.
2. Apparently the liquidus Cr-LC (the curve AB in Fig. 30) is also established sufficiently reliably^[18,62]; however the position of point B probably will be refined. The shape of the liquidus AB is confirmed by Ref.^[118] where the equilibrium curve Cr-LC for the system PBG-benzyl alcohol has the same shape. This result has a fundamental significance because it unambiguously evidences that the PBG melt is a thermotropic liquid crystal whose melting temperature decreases in the presence of the solvent.
3. There is no doubt, from our point of view, in the existence of a crystallosolvate phase, its identification with the earlier so-called “complex phase” and establishment of the corresponding polymer concentration ($V_2^{CS} = 66.7\%$).^[62–64]
4. It seems that the shape of the liquidus CS-LC (BD curve) is close to the true one up to the triple point D (although positions of the curve and point D depend on molecular mass^[64]).
5. Reliably, many authors (Refs.^[52–57,62–64,97,99] etc.), established the existence of the narrow two-phase corridor with some tilt toward higher concentrations.

masses, with extrapolation to higher values. The second way is to use very quick (“shock”) heating so the decay of the polymer does not take place during the melting. Determination of the transition temperature into the liquid phase will give the reference end point to both branches of the narrow biphasic corridor.

3. Practically not studied is the equilibrium between crystallosolvate and crystalline phases. Their common state must be determined, though the large relaxation times can complicate the real characterization.
4. The quick (“shock”) heating of pure crystallosolvate phase can help the determination of its congruent melting temperature $T_{CS \rightarrow LC}$.
5. Note, also, the importance of determination of transition temperatures of the LC phase into the narrow biphasic region at high concentrations. In other words, it is important to establish the “bending” of this corridor with increase in concentration up to $V_2 = 100\%$, where both corridor branches meet in the point A' . This is one more important confirmation of the concept of thermotropicity of the considered systems.

In this case the narrow biphasic region can be considered as the region of coexistence of a thermotropic (but not lyotropic as is usually agreed) LC phase diluted by the solvent and an isotropic liquid phase. The left (or upper) branch of this corridor can be considered as the liquidus curve between the thermotropic LC phase and isotropic phase.

6. In our mind a more detailed study of the effect of polymer molecular mass (or axial ratios of rods) on the shape and position of liquiduses CS-isotropic liquid and CS-LC is necessary. In particular, of some interest is the systematic study of molecular mass effects on the changes in shapes of the phase equilibrium curves CS-isotropic liquid (from the horizontal step to vertical ledge) and also on the changes in the T_1 and T_2 temperatures. Also desirable are more detailed studies of the “bending” shape of the biphasic corridor; at V_2^{CS} this shape may result in peculiarities in the points E and K (see Fig. 31).
7. For completeness of the picture in the region of the lowest temperatures and concentrations in Fig. 31 the liquidus curve between the crystalline state of DMF and isotropic liquid (though it practically will coincide with the temperature axis) and the region of solid solution of DMF crystals and crystallosolvates are plotted.

It is natural that some of the considered questions in this section are only hypothetical. Nevertheless, the carried-out consideration may be useful for a better understanding of the complicated combination of phase equilibria, kinetics effects, and thermal prehistory on the shape of real phase diagrams.

One may also express a careful optimism suggesting that the question of the complete view of the experimental phase diagram PBG-solvent can be resolved in relation to the synthesis of para-substituted poly(γ -benzyl-L-glutamate)^[121]; it shows a thermotropic liquid crystallinity both in the pure 100% state and in solutions, and in so doing, as is important, in the temperature range much lower than the possible degradation temperature.

6. CONCLUSION

A critical analysis of the theoretical and experimental data available in the literature allows us to suggest a new phase diagram of the PBG-DMF system in the entire concentration range as the most prominent example of the most extensively studied system of the mesogenic rigid-chain polymer-solvent type. A special role in the phase diagram belongs to crystallosolvates, which are identified with a “complex” phase described in the literature. The presence of crystallosolvates explains the pattern of changes in various properties of the PBG-DMF system (optical and rheological characteristics, aggregate and phase states) during the passage through the corresponding concentration interval.

The existence of crystallosolvates also accounts for the formation of thermoreversible gels in which crystallosolvates play the role of network nodes. Suggested classification of conventional structure units in PBG-DMF systems at high concentrations and quantitative evaluations of the fractions of these units in various ranges of the phase diagram allows to clarify the physical meaning of some phase transitions and corresponding special points and equilibrium curves in phase diagrams.

Analysis of the effect of polymer molecular mass on the liquidus curves CS-LC and CS-isotropic solution explains some peculiarities of phase diagrams in the area of low concentrations.

Experimental verification of the Flory and Onsager—Khokhlov theories, developed for description of the solutions of rigid rodlike macromolecules, is possible only within the narrow biphasic corridor in the phase diagram. Most of the remaining part of the phase diagram is complicated by processes, such as gel formation, crystallization, and crystallosolvate formation, not described by the above theories.

We should do justice, however, to Flory's phase diagram, which was obtained on the base of a lattice model. Flory emphasized repeatedly the conventional character of his PD. Nevertheless, despite its discrepancies with many details of the experimental phase diagram considered here, it undeniably has played that positive role which was predestined? to it by Flory himself, and during almost 30 years was the only theoretical guide for researchers studying liquid crystalline solutions of polymers.

REFERENCES

1. Papkov, S.P. *Phase Equilibria in the Polymer–Solvent System (in Russian)*; Chimiya: Moscow, 1981.
2. Plate, N.A., Ed.; *Liquid–Crystalline Polymers (in Russian)*; Chimiya: Moscow, 1988.
3. Papkov, S.P. Phase Equilibria in Polymer Systems, Comprising Liquid–Crystalline Phase. In Ref. [2]. Ch. 2. P. 43–72.
4. Gordon, M.I., Plate, N.A., Ed.; *Liquid crystal polymers. Advances in Polymer Science. N59*; Springer-Verlag: Berlin-Heidelberg-NY-Tokyo, 1984.
5. Papkov, S.P. *Physico-Chemical Bases of the Polymer Solution Processing (in Russian)*; Chimiya: Moscow, 1971.



6. Ciferri, A. Spinning from lyotropic and thermotropic liquid crystalline systems. In *Developments in Oriented Polymers, V.2.*; Ward, I.M., Ed.; Elsevier Applied Sci. England: London, New York, 1987; 79–113.
7. Volochina, A.V.; Kudryavtsev, G.I. High Strength and High Modulus Fibers from the Liquid–Crystalline Polymers. In Ref. [2]. Ch. 10. 372–407.
8. Frenkel, S.Ya.; Vlasov, G.P.; Ginzburg, B.M.; Shepelevskii, A.A.; Ovsyannikova, L.A.; Sokolova, T.A.; Ivanova, E.V.; Magdalev, E.T.; Volosatov, V.N.; Brestkin, Yu.V.; Belnikevich, N.G. Polymer Composition with the Cholesteric Liquid Crystalline Structure and the Method of Its Preparation. Patent of the USSR N 630898. State Register of Inventions, 1978, 7-th of July with the Priority at 1976, 14-th of June.
9. Tsutsui, T.; Tanaka, T. Polymerization of N,N-dimethylacrylamide in cholesteric mesophase. *J. Polym. Sci., Pol. Lett. Ed.* **1977**, *15* (8), 475–479.
10. Tsutsui, T.; Tanaka, R.; Tanaka, T. Liquid crystalline order in polymer composites prepared from poly(γ -benzyl-L-glutamate)-butyl acrylate liquid crystalline system. *J. Polym. Sci., Pol. Lett. Ed.* **1979**, *17* (8), 511–521.
11. Tsutsui, T.; Tanaka, R.; Tanaka, T. Topological polymer networks retaining cholesteric liquid crystalline order without mesogenes. *Mol. Cryst. Liq. Cryst. (Lett.)* **1979**, *56* (2), 57–61.
12. Nakajima, A.; Kugo, K.; Hayashi, T. Mechanical properties and water permeability of ABA tri-block copolymer membranes consisting of poly(γ -benzyl-L-glutamate) as the A-component and polybutadiene as the B-component. *Polym. J.* **1979**, *11* (12), 995–1001.
13. Sumimoto, H.; Hashimoto, K. Polyamides as barrier materials. *Adv. Polym. Sci.* **1985**, *N64*, 63–91.
14. Bouligand, Y. Liquid crystalline order in biological materials. In *Liquid Crystalline Order in Polymers*; Blumstein, A., Ed.; Academic Press: N.Y., 1978; Chap. 8.
15. Brown, G.H.; Wolken, J.J. *Liquid Crystals and Biological Structures*; Acad. Press: NY, 1979.
16. Iizuka, E. *Properties of Liquid Crystals of Polypeptides. Advances in Polymer Science. N20*; Springer-Verlag: Berlin-Heidelberg-NY-Tokyo, 1976; P79–107.
17. Samulski, E.T. Liquid crystalline order in polypeptides. In *Liquid Crystalline Order in Polymers*; Blumstein, A., Ed.; Academic Press: NY, 1978; Chap. 5.
18. Uematsu, I.; Uematsu, Y. Polypeptide liquid crystals. *Adv. Polym. Sci.* **1984**, *N59*, 37–73.
19. Papkov, S.P.; Kulitchichin, V.G. *Liquid Crystalline State of Polymers (in Russian)*; Chimiya: Moscow, 1977.
20. Elliott, A.; Ambrose, E.J. Evidence of chain folding in polypeptides and proteins. *Disc. Faraday Soc.* **1950**, *N9*, 246–251.
21. Robinson, C. Liquid crystalline structures in solutions of a polypeptide. *Trans. Faraday Soc.* **1956**, *52* (4), 571–592.
22. Robinson, C.; Ward, I.C.; Beevers, R.B. Liquid crystalline structure in polypeptide solutions P.2. *Disc. Faraday Soc.* **1958**, *N25*, 29–42.
23. Robinson, C. Liquid crystalline structures in polypeptide solutions. *Tetrahedron* **1961**, *13* (1–3), 213–234.



24. Robinson, C. The cholesteric phase in polypeptide solutions and biological structures. *Mol. Cryst.* **1966**, *1* (4), 467–494.
25. Onsager, L. The effects of shape on the interaction of colloidal particles. *Ann. NY Acad. Sci.* **1949**, *51* (4), 627–659.
26. Isihara, A. Theory of anisotropic colloidal solutions. *J. Chem. Phys.* **1951**, *19* (9), 1142–1147.
27. Flory, P.J. Statistical thermodynamics of semi-flexible chain molecules. *Proc. R. Soc. Lond., A.* **1956**, *234* (1), 60–72.
28. Flory, P. Phase equilibria in solutions of rodlike particles. *Proc. R. Soc. Lond. Ser. A* **1956**, *234* (1), 73–89.
29. Flory, P.J. *Principles of Polymer Chemistry*; Cornell University Press: Ithaca, NY, 1953.
30. Volchek, B.Z.; Purkina, A.V.; Lebedev, G.A.; Vlasov, G.P.; Ovsyannikova, L.A. Determination of geometrical asymmetry of poly(γ -benzyl-L-glutamate) molecules and its aggregations. *Vysokomol. Soed., Ser. B.* 1980, *22* (1), 25–28.
31. Baranov, V.G.; Frenkel, S.Ya.; Bi, Z.-C.; Volkov, T.I. Reversible orientational melting in solution of helical polypeptide. *Vysokomol. Soed.* **1966**, *8* (5), 957–958.
32. Shaltyko, L.G.; Shepelevskii, A.A.; Frenkel, S.Ya. Isothermal structure formation and temperature changes of quasi-equilibria supermolecular order in concentrated solutions of poly(γ -benzyl-L-glutamate). *Mol. Biol.* **1968**, *2* (1), 29–36.
33. Toriumi, H.; Kusumi, J.; Uematsu, I.; Uematsu, J. Thermally induced inversion of the cholesteric sence in lyotropic polypeptide liquid crystals. *Polym. J.* **1979**, *11* (11), 863–869.
34. Sikora, A.; Syromjatnikova, T.A.; Ginzburg, B.M.; Shepelevskii, A.A.; Frenkel, S.Ya. Temperature dependence of the pitch of the cholesteric helix of poly(γ -benzyl-L-glutamate) in N,N-dimethylformamide and N-methyl-2-pyrrolidone. *Makromol. Chem.* **1988**, *189* (1), 201–205.
35. Sobajima, S. NMR studies on orientation of liquid crystals of poly(γ -benzyl-L-glutamate) in magnetic fields. *J. Phys. Soc. Jpn* **1967**, *23* (5), 1070–1078.
36. Orwoll, R.D.; Vold, R.L. Molecular order in liquid crystalline solutions of poly(γ -benzyl-L-glutamate) in dichloromethane. *J. Am. Chem. Soc.* **1972**, *93* (21), 5335–5353.
37. Iizuka, E. The effects of magnetic fields in the structure of cholesteric liquid crystals of polypeptides. *Polym. J.* **1973**, *4* (4), 401–408.
38. Duke, R.W.; DuPre, D.B. Twist elastic constant of a cholesteric polypeptide liquid crystal. *J. Chem. Phys.* **1974**, *60* (7), 2759–2761.
39. Shepelevskii, A.A.; Ginzburg, B.M.; Alumyan, Yu.A.; Ovsyannikova, L.A.; Vlasov, G.P.; Frenkel, S.Ya. Behavior of cholesteric solution of poly(γ -benzyl-L-glutamate) in permanent magnet field. *Vysokomol. Soed., Ser. A.* **1986**, *28* (3), 596–601.
40. Shepelevskii, A.A.; Ginzburg, B.M.; Alumyan, Yu.A.; Ovsyannikova, L.A.; Vlasov, G.P.; Frenkel, S.Ya. Behavior of cholesteric solution of poly(γ -benzyl-L-glutamate) in electric field. *Vysokomol. Soed. Ser. A.* **1986**, *28* (8), 1614–1619.
41. Bamford, C.H.; Elliott, A.; Hanby, W.E. *Synthetic Polypeptides*; Academic Press Inc.: NY, 1956.
42. Bamford, C.H.; Hanby, W.E.; Happey, F. The structure of synthetic polypeptides. I. X-ray investigation. *Proc. R. Soc. Lond., A.* **1951**, *205* (1080), 30–47.



43. Doty, P.; Bradbury, J.H.; Holtzer, A.M. Polypeptides. IV. The molecular weight configuration, and association of poly(γ -benzyl-L-glutamate) in various solvents. *J. Am. Chem. Soc.* **1956**, *78* (5), 947–954.
44. Moffitt, W.; Yang, J.T. The optical rotatory dispersion of simple polypeptides. I. *Proc. Natl. Acad. Sci.* **1956**, *42* (9), 596–603.
45. Moffitt, W. The optical rotatory dispersion of simple polypeptides. II. *Proc. Natl. Acad. Sci.* **1956**, *42* (10), 736–746.
46. Zimmel, J.M.; Wu, Ch.Ch.; Miller, W.G.; Mason, R.P. Rotation motion of rodlike poly(benzyl glutamate). *J. Phys. Chem.* **1983**, *87* (26), 5435–5443.
47. Parry, D.A.D.; Elliott, A. The structure of paracrystalline phase of poly(γ -benzyl-L-glutamate) in dimethylformamide. *J. Mol. Biol.* **1967**, *25* (1), 1–13.
48. Grosberg, A.Yu. The theory of cholesteric mesophase in the solution of chiral molecules. *Doklady Akademii Nauk—Proc. Russ. Acad. Sci.* **1980**, *253* (6), 1370–1372.
49. McKinnon, A.J.; Tobolsky, A.V. Structure and properties of poly(γ -Benzyl-L-glutamate) cast from dimethylformamide. *J. Phys. Chem.* **1968**, *72* (4), 1157–1161.
50. McKinnon, A.J.; Tobolsky, A.V. Structure and transition in the solid state of a helical macromolecule. *J. Phys. Chem.* **1966**, *70* (5), 1453–1456.
51. Saba, R.G.; Sauer, J.A.; Woodward, A.E. Dynamic shear behavior of poly(γ -benzyl-L-glutamate), poly(D,L-propylene oxide), and poly(ethyl vinyl ether). *J. Polym. Sci. A.* **1963**, *1* (5), 1483–1490.
52. Bradbury, J.H.; Fenn, M.D.; Gosney, I. The change in volume associated with the helix-coil transition in poly(γ -benzyl-L- glutamate). *J. Mol. Biol.* **1965**, *11* (1), 137–140.
53. Parsons, D.F.; Martins, Y. Determination of the α -helix configuration of poly(γ -benzyl-L-glutamate) by electron diffraction. *J. Mol. Biol.* **1964**, *10* (3), 530–533.
54. Wee, E.L.; Miller, W.G. Liquid crystal-isotropic phase equilibria in the system poly(γ -benzyl-L-glutamate)-dimethylformamide. *J. Phys. Chem.* **1971**, *75* (10), 1446–1452.
55. Miller, W.G. Stiff chain polymer lyotropic liquid crystals. *Ann. Rev. Phys. Chem.* **1978**, *N29*, 519–535.
56. Miller, W.G.; Kou, L.; Tohyama, K.; Voltaggio, V. Kinetic aspects of the formation of the ordered phase in stiff-chain helical polyamino acids. *J. Polym. Sci., Polym. Symp.* **1978**, *N65*, 91–106.
57. Miller, W.G.; Wu, L.L.; Wee, E.L.; Santee, G.L.; Rai, J.H.; Goebel, K.D. Thermodynamics and dynamics of polypeptide liquid crystals. *Pure Appl. Chem.* **1974**, *38* (1–2), 37–58.
58. Wee, E.L.; Miller, W.G. In *Liquid Crystals and Ordered Fluids*, V.3. Johnson, J.F., Porter, R.S., Eds.; Plenum Press: NY, 1978; Vol. 2.
59. Miller, W.G.; Rai, J.H.; Wee, E.L. In *Liquid Crystals and Ordered Fluids*; Johnson, J.F., Porter, R.S., Eds.; Plenum Press: NY, 1974; Vol. 2, 243–255.
60. Russo, P.S.; Miller, W.G. On the nature of the poly(γ -benzyl glutamate)-dimethylformamide “complex phase”. *Macromolecules* **1984**, *17* (7), 1324–1331.
61. Watanabe, J.; Kishida, H.; Uematsu, I. *Polym. Prep. Jpn* **1981**, *30* (2), 279.

62. Ginzburg, B.M.; Syromyatnikova, T.A.; Frenkel, S.Ya.; Vlasov, G.P.; Ovsyannikova, L.A.; Rudkovskaja, G.D.; Schabsels, B.M.; Ivanova, R.A. Gel formation in poly(γ -benzyl-L-lutamate)/dimethylformamide system. *Vysokomol. Soed., Ser. B.* **1985**, *27* (10), 747–752.
63. Syromyatnikova, T.A.; Saprykina, N.N.; Schtager, V.V.; Ginzburg, B.M.; Frenkel, S.Ya. On the structure of gels from poly(γ -benzyl-L-glutamate) with dimethylformamide. *Vysokomol. Soed., Ser. B.* **1985**, *27* (4), 245–246.
64. Syromyatnikova, T.A. Liquid–crystalline state in solutions of poly(γ -benzyl-L-glutamate) and its block-copolymers Ph.D. Thesis, Institute of High Molecular Compounds, St. Petersburg, 1986.
65. Power, J.C., Jr. The aggregation of poly(γ -benzyl-L-glutamate) in mixed solvent systems. In *Liquid crystals and ordered fluids*; Johnson, J.F., Porter, R.S., Eds.; Plenum Press: N.Y.-London, 1970; 365–373.
66. Khokhlov, A.R. Statistical physics of liquid crystalline ordering in polymer systems. In Ref. [2], Ch. 1. pp. 7–42.
67. Birshstein, T.M.; Kolegov, B.I.; Pryamitsyn, V.A. On the theory of athermic lyotropic liquid crystalline systems. *Vysokomol. Soed., Ser. A.* **1988**, *30* (2), 348–354.
68. Khokhlov, A.R. On the formation conditions of liquid crystalline phase in solutions of absolutely rigid macromolecules. *Vysokomol. Soed., Ser. A.* **1979**, *21* (9), 1981–1989.
69. Grosberg, A.Yu.; Khokhlov, A.R. Statistical theory of polymeric lyotropic liquid crystals. *Speciality Polymers*; Springer: Berlin, 1981; 53–97.
70. Khokhlov, A.R.; Semenov, A.N. Liquid–crystalline ordering in the solution of long persistent chains. *Physica A* **1981**, *108* (2–3), 546–556.
71. Khokhlov, A.R. Liquid–crystalline ordering in the solution of semiflexible macromolecules. *Phys. Lett. A* **1978**, *68* (1), 135–136.
72. Valenti, B.; Sartirana, M.L. Mesophase formation in lyotropic polymers. *Il Nuovo Cimento, D.* **1984**, *3* (1), 104–120.
73. Balbi, C.; Bianchi, E.; Ciferri, A.; Tealdi, A.; Krigbaum, W.R. Equilibria of extended-chain polymers and liquid–crystalline phases. *J. Polym. Sci., Polym. Phys. Ed.* **1980**, *18* (10), 2037–2053.
74. Papkov, S.P. On the mutual combination of liquid, liquid crystalline, and crystalline phase equilibria in the relation of the morphology problem of natural polymers. *Vysokomol. Soed., Ser. A.* **1984**, *26* (5), 1083–1089.
75. Papkov, S.P. Phase equilibria in rigid-chain polymer systems. In *Contemporary Topics in Polymer Science*; Pearce, E.M., Schaefgen, J.R., Eds.; Plenum Press: New York, 1977; Vol. 2, 97–108.
76. Papkov, S.P. Liquid crystalline order in solutions of rigidchain polymers. In: Ref. [4]. 75–102.
77. Warner, M.; Flory, P.J. The phase equilibria in thermotropic liquid–crystal systems. *J. Chem. Phys.* **1980**, *73* (12), 6327–6332.
78. Counsell, C.; Warner, M. A new theory of nematic liquid–crystal mixtures. *Mol. Cryst. Liq. Cryst.* **1983**, *100* (3–4), 307–326.
79. Ciferri, A. Rigid and semirigid chain polymeric mesogens. In *Polymer Liquid Crystals*; Ciferri, A., Krigbaum, W.R., Meyer, R.B., Eds.; Academic Press: New York, 1982; 63–102.



80. Papkov, S.P. Diagram of state rigid-chain polymer/solvent with incongruent melting of crystallosolvate. *Vysokomol. Soed., Ser. B.* **1982**, *24* (2), 109–112.
81. Papkov, S.P. Diagram of state of the PBA/H₂SO₄ system. *Vysokomol. Soed., Ser. B.* **1979**, *21* (10), 787–791.
82. Hermans, J., Jr. The viscosity of concentrated solutions of rigid rodlike molecules poly(γ -benzyl-L-glutamate) in m-cresol. *J. Colloid Sci.* **1962**, *17* (7), 638.
83. Teramoto, A. Private communication. Institute of High Molecular Compounds: St.-Petersburg, 1994.
84. Volchek, B.Z.; Purkina, A.V.; Lebedev, G.A.; Vlasov, G.P.; Ovsyannikova, L.A. Experimental study of the phase equilibria liquid crystal— isotropic solution of poly(γ -benzyl-L-glutamate) different solvents. *Vysokomol. Soed., Ser. A.* **1980**, *22* (4), 841–849.
85. Kiss, G.; Porter, R. Rheology of concentrated solutions of poly(γ -benzyl-glutamate). *J. Polym. Sci. Polym. Symp.* **1978**, *N65*, 193–211.
86. Nakajima, A.; Hayashi, T.; Ohnori, M. Phase equilibria of rod-like molecules in binary solvent systems. *Biopolymers* **1968**, *6* (7), 973–982.
87. Flory, P.J. Molecular theory of liquid crystals. In: Ref. [4]. 1–35.
88. Helfrich, J.; Hentschke, R.; Apel, U.M. Molecular dynamics simulation study of poly(γ -benzyl-L-glutamate) in dimethylformamide. *Macromolecules* **1994**, *27* (2), 472–482.
89. Schmidt, M. Combined integrated and dynamic light scattering by poly(γ -benzyl-glutamate) in a helicogenic solvent. *Macromolecules* **1984**, *17* (4), 553–560.
90. Ookubo, N.; Komatsubara, M.; Nakajima, H.; Wada, Y. Infinite dilution viscoelastic properties of poly(γ -benzyl-L-glutamate) in m-cresol. **1976**, *15* (5), 929–947.
91. Tsvetkov, V.N.; Mitin, Yu.V.; Shtennikova, I.N.; Gluschenkova, V.R.; Tarasova, G.V.; Skazka, V.S.; Nikitin, N.A. Sedimentation, diffusion, and viscosity of poly(γ -benzyl-L-glutamate) in solutions. *Vysokomol. Soed.* **1965**, *7* (6), 1098–1103.
92. Tsvetkov, V.N.; Shtennikova, I.N.; Ryumtsev, E.I.; Ochrimenko, G.I. Flow birefringence and optical anisotropy of poly(γ -benzyl-L-glutamate) molecules in solutions. *Vysokomol. Soed.* **1965**, *7* (6), 1104–1110.
93. Tsvetkov, V.N.; Shtennikova, I.N.; Ryumtsev, E.I.; Skazka, V.S. Birefringence in electric field, rotational diffusion, and dipole moment of poly(γ -benzyl-L-glutamate) molecules in solutions. *Vysokomol. Soed.* **1965**, *7* (6), 1111–1116.
94. Straley, J.P. The gas of long rods as a model for lyotropic liquid crystals. *Mol. Cryst. Liq. Cryst.* **1973**, *22* (3–4), 333–357.
95. Papkov, S.P. Liquid–crystalline state of linear polymers. *Vysokomol. Soed., Ser. A.* **1977**, *19* (1), 3–18.
96. Sokolova, T.S.; Efimova, S.G.; Volochina, A.V.; Kudryavtsev, G.I.; Papkov, S.P. Transition of sulfuric acid solutions of poly(p-phenylene terephthalamide) in anisotropic state. *Vysokomol. Soed., Ser., A.* **1973**, *15* (11), 2501–2505.
97. Volchek, B.Z.; Purkina, A.V.; Vlasov, G.P.; Ovsyannikova, L.A. On the temperature dependence of the concentration boundaries of the existence of liquid crystalline phase in solutions of stiff-chain polymers. *Vysokomol. Soed., Ser. B.* **1981**, *23* (2), 154–157.



98. Ginzburg, B.M.; Syromyatnikova, T.A.; Frenkel, S.Ya. Gelation of poly(γ -benzyl-L-glutamate)/dimethylformamide system. *Polym. Bull.* **1985**, *13* (2), 139–144.
99. Volchek, B.Z.; Purkina, A.V.; Merkur'eva, A.A.; Vlasov, G.P.; Ovsyannikova, L.A. Experimental study of the state diagrams of the concentrated solutions of stiff-chain polymers with the different rigidity of macromolecules. *Vysokomol. Soed., Ser. A.* **1984**, *26* (4), 711–715.
100. Flory, P.; Ronca, G. Theory of systems of rodlike particles. *Mol. Cryst. Liq. Cryst.* **1979**, *54* (3–4), 289–309.
101. Flory, P.J.; Ronca, G. Theory of systems of rodlike particles. II. Thermotropic systems with orientation-dependent interactions. *Mol. Cryst. Liq. Cryst.* **1979**, *54* (3–4), 311–330.
102. Russo, P.S.; Miller, W.G. Coexistence of liquid crystalline phases in poly(γ -benzyl-L-glutamate)-dimethylformamide. *Macromolecules* **1983**, *16* (11), 1690–1693.
103. Luzzati, V.; Cesary, M.; Spah, G.; Masson, F.; Vincent, J.M. La structure du poly-L- γ -glutamate de benzyle en solution. Configuration en helice differente de L' helice let transitions entre formes helicoidales. *J. Mol. Biol.* **1961**, *3* (5), 266–284.
104. Squire, J.M.; Elliott, A. Liquid crystalline phases of poly(γ -benzyl-L-glutamate) in solution. *Mol. Cryst. Liq. Cryst.* **1969**, (7), 457–468.
105. Tohyama, K.; Miller, W.G. Network structure in dets of rodlike polypeptides. *Nature* **1981**, *289* (5800), 813–814.
106. Miller, W.G. Aggregation, phase behavior, and the nature of networks formed by some rodlike polymers. In *Microdomains in Polymer Solutions*; Dubin, P.L., Ed.; Plenum Press: NY, London, 1984.
107. Blout, E.R.; Kurlson, R.H. Polypeptides. III. The synthesis of high molecular weight poly- γ -benzyl-L-glutamates. *J. Am. Chem. Soc.* **1956**, *78* (5), 941–947.
108. Vlasov, G.P.; Rudkovskaya, G.D.; Ovsyannikova, L.A. Synthesis of block copolymers containing a carbon chain and a polypeptide block. *Macromol. Chem.* **1982**, *183* (11), 2635–2644.
109. Sekiguchi, H. Kinetics and mechanism of ϵ -caprolactone anionic polymerization under the influence of amines. *Pure Appl. Chem.* **1981**, *53* (9), 1689–1714.
110. Ballard, D.G.H.; Bamford, C.H. Studies of polymerization. VII. The polymerization of N-carboxy- α -amino acid anhydrides. *Proc. Roy. Soc. Lond. Ser. A.* **1954**, *223* (1155), 495–520.
111. Ginzburg, B.M.; Korzhavin, L.N.; Frenkel, S.Ya.; Lajus, L.A.; Adrova, N.A. Crystallinity of Poly-2,2'-octamethylene-5,5'-dibenzimidazole. *Vysokomol. Soed.* **1966**, *8* (2), 278–281.
112. Frenkel, S.Ya.; Ginzburg, B.M. Crystallinity of Poly-2,2'-octamethylene-5,5'-dibenzimidazole and structural changes resulting from the heat treatment. *J. Polym. Sci., C.* **1969**, *N22*, 813–823.
113. Iovleva, M.M.; Smirnova, V.N.; Chanin, Z.S.; Volochina, A.V.; Papkov, S.P. About the determination of melting temperatures of polymer crystallosolvates by the measurements of the turbidity of the system. *Vysokomol. Soed., Ser. A.* **1981**, *23* (8), 1867–1871.
114. Iovleva, M.M.; Papkov, S.P. Polymer crystallosolvates. *Vysokomol. Soed., Ser. A.* **1982**, *24* (2), 233–248.



115. Iovleva, M.M.; Banduryan, S.N.; Ivanova, N.A.; Platonov, V.A.; Mil'kova, L.P.; Chanin, Z.S.; Volochina, A.V.; Papkov, S.P. On the spherulites of poly-p-phenylene-terephthalamide. *Vysokomol. Soed., Ser. B.* **1979**, *21* (5), 351–354.
116. Park, J.-Y.; Kim, D.; Harris, F.W.; Cheng, S.Z.D. Phase structure, morphology and phase boundary diagram in an aromatic polyamide (BPDA-PFMB)/m-cresol system. *Polym. Int.* **1995**, *37* (3), 207–214.
117. Demus, D.; Zschke, H.; *Flussige kristalle in tabellen.* VEB Dtsch. Verl. Grundstoffind, Leipzig, 1974.
118. Sasaki, Sh.; Hikata, M.; Shiraki, C.; Uematsu, I. Molecular aggregation and gelation in poly(γ -benzyl-L-glutamate) solutions. *Polym. J.* **1982**, *14* (3), 205–213.
119. Filippov, V.K.; Chernik, G.G. Heat capacity of heterogeneous systems and thermal analysis. *Termochim-Acta* **1986**, *101*, 65–75.
120. Andreeva, I.N.; Chanin, Z.S.; Romanko, O.I.; Volochina, A.V.; Iovleva, M.M.; Kalaschnik, A.T.; Papkov, S.P.; Kudryavtsev, G.I. Study of crystallosolvates of poly(p-phenylene terephthalamide). *Vysokomol. Soed., Ser. B.* **1981**, *23* (2), 89–93.
121. Iizuka, E.; Abe, K.; Hanabusa, K.; Shirai, H. Properties of thermotropic liquid crystalline poly(4-substituted- γ -benzyl-L-glutamate)s. *Curr. Top. Polym. Sci.* **1987**, *1*, 235.

Received August 31, 2001

Revised November 9, 2001

Accepted November 19, 2001